AD NUMBER

AD474925

NEW LIMITATION CHANGE

TO

Approved for public release, distribution unlimited

FROM

Distribution authorized to U.S. Gov't. agencies and their contractors; Critical Technology; DEC 1965. Other requests shall be referred to Rome Air Development Center, ATTN: EMATE, Griffiss AFB, NY 13441-5700.

AUTHORITY

RADC ltr dtd 17 Sep 1971

SECURITY MARKING

The classified or limited status of this report applies to each page, unless otherwise marked.
Separate page printouts MUST be marked accordingly.

THIS DOCUMENT CONTAINS INFORMATION AFFECTING THE NATIONAL DEFENSE OF THE UNITED STATES WITHIN THE MEANING OF THE ESPIONAGE LAWS, TITLE 18, U.S.C., SECTIONS 793 AND 794. THE TRANSMISSION OR THE REVELATION OF ITS CONTENTS IN ANY MANNER TO AN UNAUTHORIZED PERSON IS PROHIBITED BY LAW.

NOTICE: When government or other drawings, specifications or other data are used for any purpose other than in connection with a definitely related government procurement operation, the U. S. Government thereby incurs no responsibility, nor any obligation whatsoever; and the fact that the Government may have formulated, furnished, or in any way supplied the said drawings, specifications, or other data is not to be regarded by implication or otherwise as in any manner licensing the holder or any other person or corporation, or conveying any rights or permission to manufacture, use or sell any patented invention that may in any way be related thereto.

RADC-TR- 65-188
Final Report

EXPERIMENTAL AIRBORNE MICROWAVE SUPPORTED PLATFORM

W. C. Brown

TECHNICAL REPORT NO. RADC-TR- 65- 188

December 1965

DA-64-14

Techniques Branch
Rome Air Development Center
Research and Technology Division
Air Force Systems Command
Griffiss Air Force Base, New York

When US Government drawings, specifications, or other data are used for any purpose other than a definitely related government procurement operation, the government thereby incurs no responsibility nor any obligation whatsoever; and the fact that the government may have formulated, furnished, or in any way supplied the said drawings, specifications, or other data is not to be regarded, by implication or otherwise, as in any manner licensing the holder or any other person or corporation, or conveying any rights or permission to manufacturer, use, or sell any patented invention that may in any way be related thereto.

Do not return this copy. Retain or destroy.

EXPERIMENTAL AIRBORNE MICROWAVE SUPPORTED PLATFORM

W. C. Brown

FOREWORD

This report was prepared by the Spencer Laboratory of the Raytheon Company, under Contract AF30(602)-3481 covering the period June 64-April 65. The work was under the general direction of Mr. W. C. Brown, Manager of the Super Power Operation of the Microwave & Power Tube Division of the Raytheon Company. Mr. Brown also acted as project engineer, assisted by Mr. J. R. Mims and Mr. N. I. Heenan. Mr. Mims was responsible for the mechanical engineering aspects and Mr. Heenan contributed to the design of the microwave beam.

This investigation was supported by the Laboratory Directors' (Discretionary) Funds. RADC Project Monitor was R. Hunter Chilton (EMATE).

This technical report has been reviewed and is approved.

Approved: ARTHUR J. FROHLICH
Chief, Techniques Branch
Surveillance & Control Division

Approved: THOMAS S. BOND, Jr
Colonel, USAF
Chief, Surveillance &
Control Division

FOR THE COMMANDER:

IRVING J. GABELMAN
Chief, Advanced Studies Group

ABSTRACT

Microwave power transmission and helicopter technologies have been successfully combined to produce a hovering vehicle which is held aloft solely by power derived from a microwave beam. New, efficient, and lightweight antenna and rectifier technologies allow the helicopter to support its energy-capture system and a substantial payload in addition to its own weight. In more detail, a microwave-powered helicopter with a six-foot rotor has been flown at an altitude of fifty feet for ten continuous hours. The helicopter was kept over the microwave beam by means of a suitable tethering system.

TABLE OF CONTENTS

LIST OF ILLUSTRATIONS

LIST OF ILLUSTRATIONS (Continued)

LIST OF ILLUSTRATIONS (Continued)

LIST OF ILLUSTRATIONS (Continued)

EVALUATION

1. The program for a microwave supported platform was initiated to establish the feasibility of transmitting large amounts of energy via beamed microwaves and then converting to useable dc. This was to be demonstrated by using the dc to power a small airborne platform. Heretofore microwaves had been rectified under idealized laboratory conditions with heavy unreliable vacuum devices handling reasonable amounts of rf and by solid state diodes rectifying less than a milliwatt of power. Rectified microwave energy had never been used as the power source for other equipment.

2. The contractor approached the task by using existing technology and economical components and not by new major developments in any one area. The result was a six pound system consisting of an array of 4000 odd solid state diodes that acted as both receiving antenna and rectifier and a small drill motor to drive a six foot balsa wood rotor. Tethers restricted the platform to the vertical axis where it fulfilled contractual requirements by flying at 50 feet above the transmitting antenna for 10 hours.

3. It should be emphasized that this was a feasibility effort. Before the system can be used in proposed applications, much work remains. The efficiency of the rectifying antenna must be improved and the helicopter will have to be capable of remaining in position independent of tethers. With these improvements and the current state of the art of microwave power generation, it should be possible to transfer sufficient energy to provide power required for the platform as well as a surveillance or communication system on board at a height several thousand feet above the ground.

4. The helicopter and rectifying antenna built and tested on this program is currently being shown in the "Federal Science and Engineering Exhibit" being displayed in the Smithsonian and other major missions around the country.

R. H. Chilton

R. H. CHILTON
Project Engineer

1.0 INTRODUCTION

A microwave-powered helicopter may be defined as a vehicle which rides on a microwave beam and extracts from the beam all the energy needed for its propulsion.

The motivation for the study and development effort leading to the microwave-powered helicopter flights described in this report is the concept of a high altitude platform which can be kept on station for periods of weeks or even months by means of a microwave beam, performing communication and other useful functions that could be associated with an extraordinarily high transmitting tower. The near-term objectives as represented by the major purpose of this study, however, have been to demonstrate that a heavier-than-air vehicle of modest size could be kept aloft solely by means of microwave energy at an altitude sufficiently great to demonstrate the beaming of microwave energy and for a time duration of sufficient length to indicate the basic reliability of the components of the system. As a result of the successful experimental flights and the favorable nature of other data that has been collected, it is reasonable to expect that high altitude microwave-powered helicopters will be developed in the future and that they will accomplish practically useful missions.

The significance of the microwave-powered helicopter development, however, extends considerably beyond its potential to provide a new and useful aerospace capability. It represents the first application of power transfer by microwave beam, an emerging technology more basic in nature and with many potential applications, but needing an initial application to speed its growth and acceptance. The microwave-powered helicopter also represents an interdisciplinary development of unusual scope which cuts across the established charters of many professional, corporate, and government organizations. It represents for the first time the penetration of microwaves into the propulsion aspects of aircraft design and into the area of aerospace component activity generally referred to as "energy sources".

The technology upon which the successful results of this present study is based is an outgrowth of projects sponsored by both government and industry. In particular, it was a direct outgrowth of a demonstration by the Raytheon Company on May 23, 1963 to personnel of the Rome Air Development Center that a microwave beam could be used for the efficient transfer of meaningful amounts of electrical power. In this experiment, the microwave energy itself was transferred with an efficiency of 51% over a distance of twenty-five feet, and then converted with an efficiency of 50% into DC power of 100 watts which was used to drive an electrical motor. In this experiment, a close-spaced thermionic diode developed by the Raytheon Company was used as the rectifier.

A few months after this demonstration in microwave power transfer, personnel of the Raytheon Company conducted experiments with an electrically powered helicopter having rotor blade diameters of four and six feet. These helicopters exhibited an excess lifting capability sufficient to carry a lightweight receiving antenna and a close-spaced thermionic diode rectifier.

With the completion of the essential microwave and airframe components, the next obvious stage of development was to combine these components and conduct an experiment in which the helicopter would be supported solely by microwave energy beamed to it. The Raytheon Company prepared an unsolicited proposal for this purpose and submitted it to the Rome Air Development Center of the Research and Technology Division of the Air Force Systems Command.

Meanwhile, the problem of the microwave receiving antenna and the microwave power rectifier had received additional study at the Raytheon Company. It was apparent that a practical aerospace application of microwave power transmission imposed severe limitations and restrictions upon the receiving antenna and the microwave power rectifier with respect to weight, directivity, cooling, efficiency, and other factors. After additional study, it was felt that the best approach to a satisfactory

aerospace antenna and rectifier was to combine these two elements into a common structure which would both capture and rectify the microwave energy and to base this approach upon the use of the point-contact silicon semiconductor diode. Extensive work at Purdue University by Prof. George and others had established that the semiconductor diode was an efficient rectifier at the lower microwave frequencies, although the power-handling capability of the device had been demonstrated to be so low that it would require literally thousands of them to produce a kilowatt of rectified power. However, it became apparent that the necessity of using thousands of these diodes is in reality an asset in an aerospace application since it affords an opportunity to deploy them in such a fashion that the antenna can be made relatively non-directional in its characteristics as well as making it possible to locate the heat sinks for disposing of the dissipated power very close to its sources.

The development of the combination antenna and rectifier as a successful approach involved combining the electrical and mechanical aspects of the development in such a way as to obtain a satisfactory ratio of power-handling capability to weight. The development proceeded rapidly and antenna modules of about twenty watts each were being constructed by the early part of 1964.

Based upon the satisfactory performance of these modules, a decision was made to abandon other approaches to aerospace receiving antennas and rectifiers, and to proceed to design a microwave helicopter based upon the new rectifying-antenna approach and the six-foot diameter helicopter rotor which had been demonstrated previously.

A microwave-powered helicopter so designed was actually flown and demonstrated to a substantial number of individuals on July 1 and 2, 1964. As is often characteristic of the first experimental performance of new devices, there was relatively little reserve power to support more than a minimum tethering system and with which to provide convincing flights at respectable altitudes, adequate rates of climb,

and of substantial duration.

The present study made it possible to make convincing demonstrations with respect to these items, and in addition accumulate information which may help with the next phase of development of the microwave-powered helicopter.

In particular, the demonstrations motivated a number of industrial companies to supply improved semiconductor diodes for test purposes. Such testing fitted in nicely with a secondary objective of the present study which was to obtain test data and establish guide lines for testing of the microwave rectifier to be employed. The performance of some of these diodes in terms of power-handling-to-weight ratio is many times that of the diodes that were successfully used in the experiment, and represents an available, "on-the-shelf" state-of-the-art improvement of the greatest importance to the further development of the microwave-powered helicopter.

Of further importance to the rapid development of the microwave-powered helicopter as a high altitude vehicle are similar "on-the-shelf" developments with respect to microwave power generation and antenna technology.

In the report which follows, the first section summarizes the work which was accomplished. The next section provides a detailed description of the major components of the microwave-powered helicopter, and the associated microwave beam. This is followed by a brief section on conclusions and recommendations. The extensive work on the testing of diodes that was performed at Purdue University under a subcontract is included in its original report form as a major appendix to the main report.

2.0 SUMMARY

A microwave-powered helicopter system consists essentially of two major parts, (1) a microwave beam system from which the microwave-powered helicopter obtains power for its support, and (2) the microwave-powered helicopter itself. The microwave beam system consists of a source of microwave power and an optical system whereby this power is focused into a narrow beam. The microwave-powered helicopter consists of a means of extracting rf energy from the microwave beam, a means of converting this energy into dc power, a dc motor, and a helicopter rotor. These various elements are shown to comprise the over-all system as shown in Figure 1.

The experiments described in this report made use of all these elements and in addition employed a tethering system which kept the helicopter positioned on the beam at all times while providing no vertical support. The over-all system is shown in Figure 2.

The microwave beam system, shown in Figure 3, made substantial use of experimental equipment that had been used for earlier investigations of efficient microwave power transfer. A magnetron oscillator generating from three to five kilowatts of power at a frequency of 2450 Mc/sec was used as the power source. A 9.5 foot diameter ellipsoidal reflector with a focal length of 52 inches was used as the beam-forming reflector. It was illuminated by means of a diagonal horn.

The microwave-powered helicopter is shown in Figure 4. The six-foot diameter rotor is driven by a universal fractional horsepower motor which is adapted from an ordinary electric drill. A special gear box employing ball bearing construction throughout is used to reduce the high shaft speed of the drill to the 400 RPM of the helicopter rotor. The rotor power for helicopter takeoff is 0.105 horsepower. The weight of the helicopter without any payload is 5.25 pounds. At the saturation level of its antenna and rectifier system, it can support a payload of 1.5 pounds.

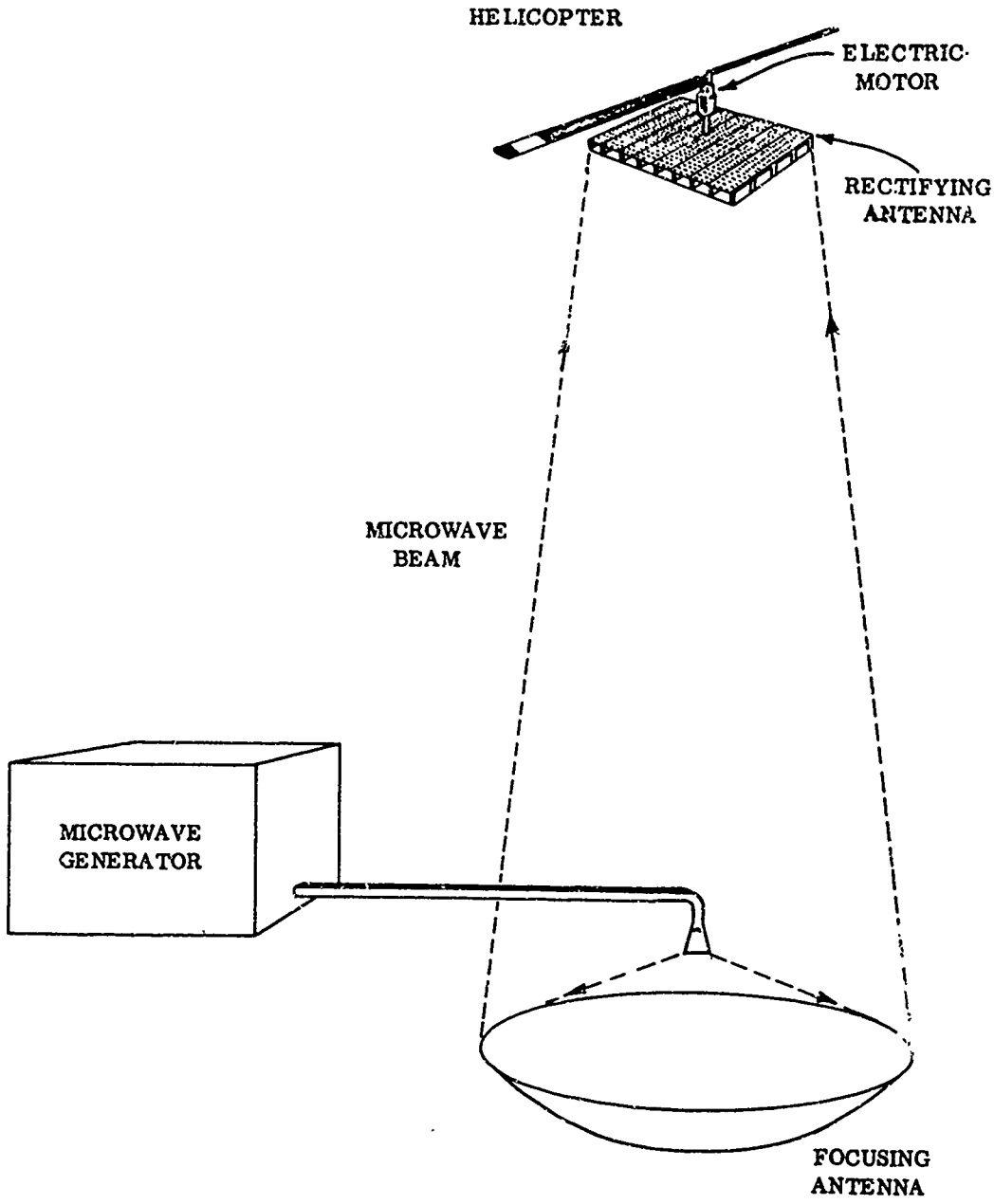

Figure 1. The Basic Elements of a Microwave-Powered Helicopter System.

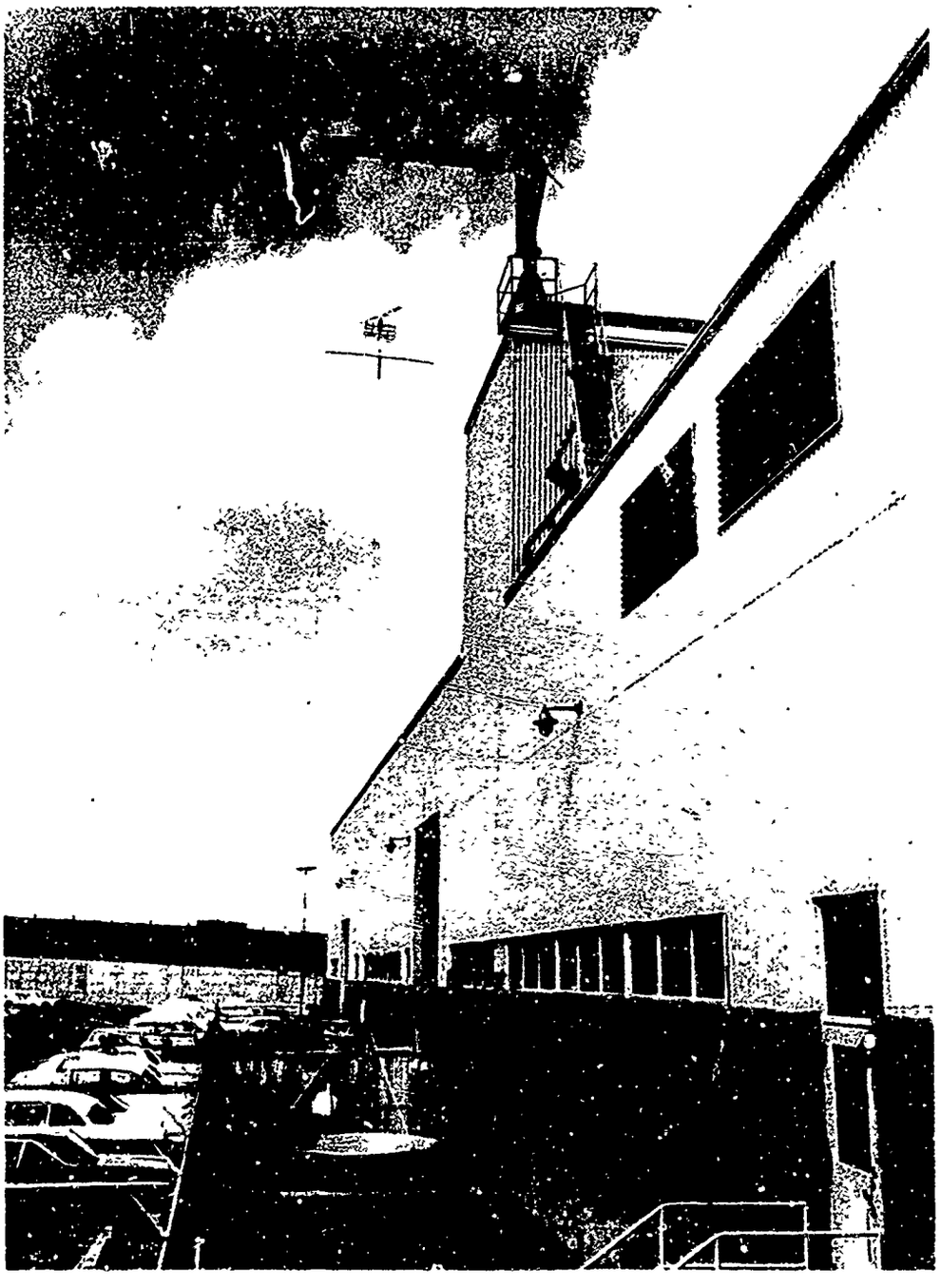

Figure 2. Experimental System Used at the Spencer Laboratory of the Raytheon Company for Flight Testing of the Microwave-Powered Helicopter

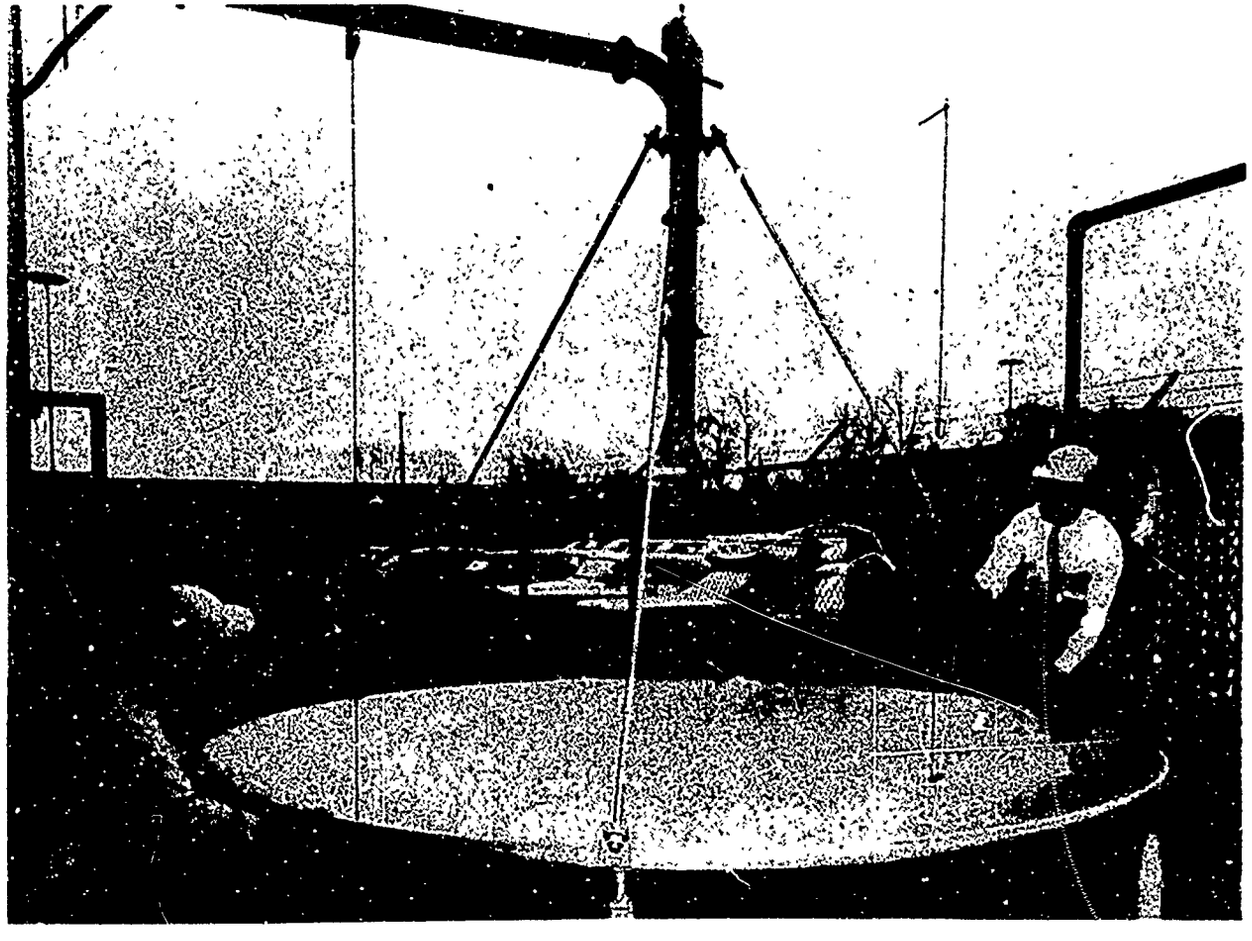

Figure 3. Antenna Feed and Ellipsoidal Reflector which Formed the Microwave Beam for the Experiment

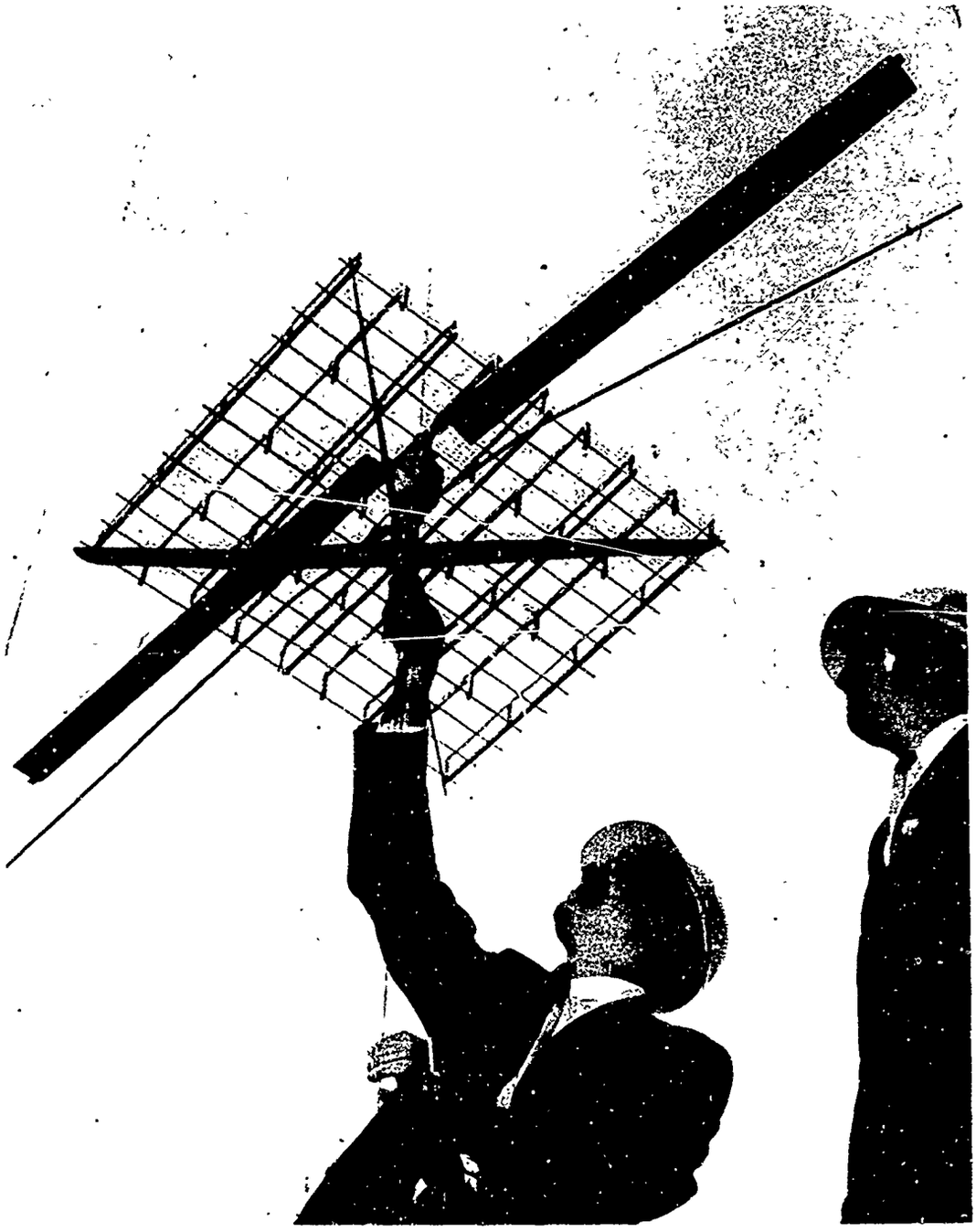

Figure 4. Close-Up View of the Microwave-Powered Helicopter Showing Combination Antenna and Rectifier, Rotor and Motor

The most novel feature of the helicopter is the combination receiving antenna and rectifier which is made up of over 4000 point-contact silicon rectifier diodes. The antenna is designed with great consideration given to keeping its weight as light as possible. The dc power output of the combination antenna and rectifier is 280 watts; 180 watts is the minimum power at which the helicopter will fly.

The microwave helciopter is shown in typical flights in Figures 2 and 5. The helicopter typically took off from its support which was located twenty-five feet from the transmitting antenna and climbed to an altitude of fifty feet. The special three-wire tethering system which was used to keep the helicopter over the beam and to supply the counter torque to prevent the body of the helicopter from spinning was held in tension between concrete posts in the ground and a heavy steel beam supported from the top of the building.

Many flights of the microwave-powered helicopter using microwave energy as the sole means of support were made, including one of ten continuous hours at an altitude of fifty feet. This flight was a required objective of the contract. There was no observable deterioration in performance after this period of operation.

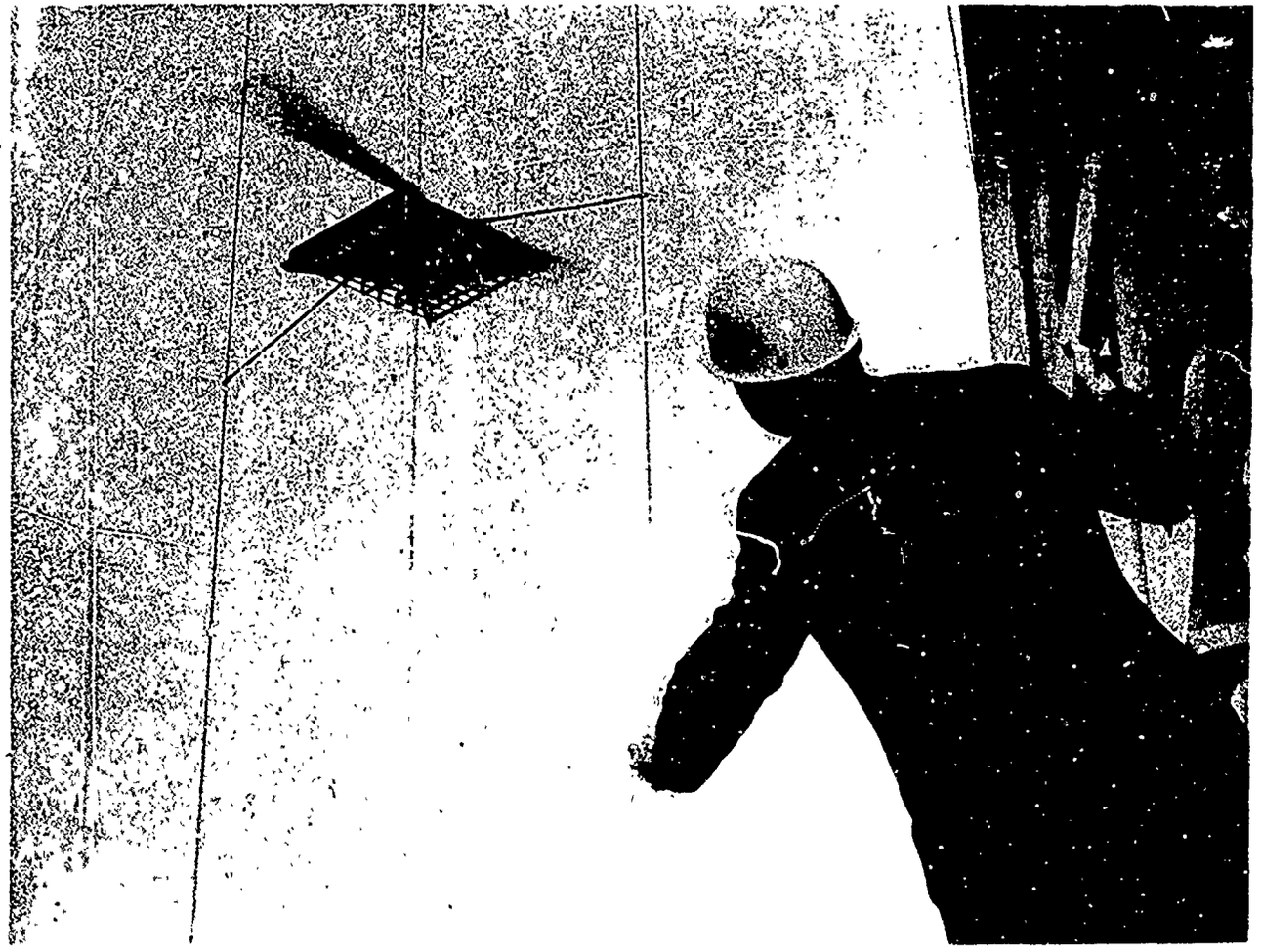

Figure 5. View of the Microwave-Powered Helicopter in Flight at an Altitude of Fifty Feet

3.0 DESCRIPTION AND PERFORMANCE OF THE MAJOR COMPONENTS OF THE MICROWAVE-POWERED HELICOPTER AND THE ASSOCIATED MICROWAVE BEAM

The microwave-powered vehicle may best be analyzed by a consideration of the major parameters that must be considered in its design. These design parameters are the rotor, the motor and necessary gearing, and the combination capture antenna and microwave rectifier.

In addition to these items a discussion of the details of the tethering approach is appropriate to this particular study. A description of the microwave beam system is also appropriately included.

3.1 HELICOPTER ROTOR DESIGN

Introduction

Helicopter rotor design may be approached from two points of view. It may be approached from the point of view that the rotor is a rotating wing with the properties of lift and drag. It may also be approached from the point of view that the function of the rotor is to impart a change of momentum with respect to time to the air flowing through the rotor thereby providing a thrust in the opposite direction equal to the momentum change.

In the following analyses we will use the change in momentum approach for the hovering helicopter. The approach, using change of momentum, is an approach applicable to all propulsion devices involving a change in the momentum of a fluid or gas, including the rocket, the turbojet, the propeller, and the helicopter rotor.

The time rate of change of the total momentum of a bounded mass system of a fluid or gas in any direction is equal to the resultant of the external forces acting on the boundaries in the specified direction.

This may be stated mathematically as --

$$\frac{d}{dt} (MV) = \Sigma F_{ext} \qquad (1)$$

where: M is the mass of the system

V is the velocity of the system.

If equation (1) is integrated, we obtain --

$$\Delta M = \int_{t_1}^{t_2} \Sigma F_{ext} \; at \qquad (2)$$

where: $\Delta M = \Delta(MV)$ and is equal to the net change in momentum.

If the external force is constant with time, then

$$\Delta M = F_{ext} t$$

or F_{ext} = change in momentum per unit time. (3)

A further understanding of the action of a rotor or propeller may be obtained by the introduction of the concept of the slip stream. Fig. 5 a (a) shows how the rotor is related to the slip stream. The contour of the slip stream is determined by the requirement that the amount of mass flowing at any point along the slip stream be constant under steady state conditions. This is equivalent to saying that the amount of mass coming out of the system per unit time is equal to the amount of mass going into the system per unit time. With a compressible fluid such as air, the mass flow is a function of the cross section of the slip stream, the velocity of flow, and the density of the stream. The density will vary as the pressure and temperature of the air.

From Fig. 5 a (b) we see that the pressure for (a) upstream of the rotor is near atmospheric. The pressure differential is low, the air is therefore accelerated slowly, the resultant velocity is low, and a large cross sectional area of the slip stream is necessary. Closer to the rotor, the pressure differential is greater, the air is moving progressively faster, and the diameter of the slip stream is smaller.

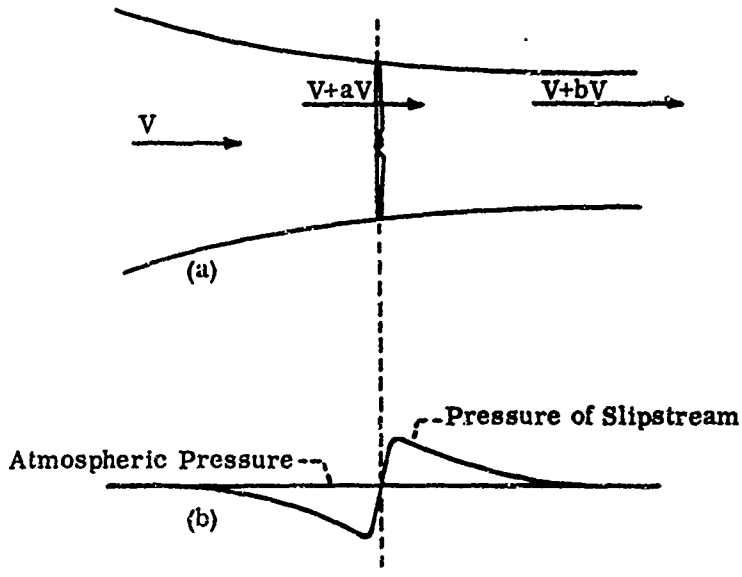

Figure 5(a). Airscrew in forward flight.

(a) Airstream velocities.
(b) Pressure distribution.

At the rotor itself, energy is added to the slip stream. Immediately above and below the rotor, the slip stream has the same diameter. Hence, the continuity of the flow of mass through the rotor demands that the air density be the same on both sides of the rotor. Energy imparted to the air must result in speeding up of the air particles. They would therefore be further apart and the density reduced if it were not for the fact that there is an abrupt increase in the pressure of the air as it goes through the rotor. This increase in the pressure of the air will act to accelerate it further in the downstream direction and will result in a further decrease in the diameter of the slip stream.

Now the work done by the rotor in one second relative to the slip stream in which it is immersed is equal to the force it exerts times its movement relative to the air in the slip stream. This is numerically equal to the thrust, T times the air velocity. The air velocity is equal to the relative velocity, V, of the machine on which the rotor is mounted with respect to the main body of the atmosphere plus the additional velocity of the slip stream which at the rotor is aV. The work done is therefore:

$$T\,(V + aV) \approx \Delta KE. \qquad (4)$$

The thrust developed by the air screw is equal to the change in the axial momentum of the air in unit time.

If A is the area of the disk and ρ the mass density of the air, the thrust developed by the rotor is --

$$T = \rho A\,(V + aV)\; bV, \quad \text{where} \qquad (5)$$

bV is the maximum change in the velocity of the air, as noted in Figure 5a(a).

The increase in kinetic energy per second, ΔKE, is simply:

$$\Delta KE = 1/2\,\dot{m}\,(V + bV)^2 - 1/2\,\dot{m}\,V^2 \qquad (6)$$

where: $\dot{m}$ is the mass flow rate, which is constant over the length of the slip stream, and can be related to the disk area as follows:

$$\dot{m} = \rho A\,(V + aV) \qquad (7)$$

If expressions (5), (6), and (7), are substituted into (4), the following relationship is obtained:

$$\left[\rho A V (1 + a)\, bV\right]\left[V (1 + a)\right] = 1/2\,\rho A V^3 (1 + a)(b^2 + 2b)$$

Solving for b in terms of a,

$$b = 2a, \qquad (8)$$

which states that the velocity imparted to the air at the rotor disk is one-half the total increase in velocity. This relationship may be of some value in the locating of the rectenna in the downwash for an optimum combination of drag and cooling.

If the helicopter is hovering with no movement with respect to the atmosphere, then $V = 0$, and the increase in velocity, aV, at the rotor disc is equal to the total velocity through the disk, or the induced velocity v. It follows from (4) and (8)

$$T = (\rho \pi R^2 v)\,(2v) \qquad (9)$$

where: R is the radius of the rotor disk.

Solving for ν

$$\nu = \sqrt{\frac{T}{2\rho\pi R^2}} \tag{10}$$

The induced velocity at the rotor is relatively low. For example, in the case of the rotor used for the microwave-powered helicopter which is the subject of this report, the rotor lift or thrust T is approximately 6 lbs. and the radius, R, is 3 feet. The air density at sea-level pressure is .002378 slugs per cubic foot. For these conditions ν is found to be 6.7 feet per second, or 4.6 miles per hour.

In the above example, the power that is represented by maintaining a thrust of 6 pounds is obtained with the aid of equations (6) and (7) with V set equal to zero, and ν substituted in place of aV. This results in --

$$\Delta KE = 2\rho A \nu^3 - 2\rho \pi R^2 \nu^3 \tag{11}$$

But ΔKE is in units of ft. lbs./sec. Equation (11) may be converted to Horsepower by dividing by 550. If this is done it is found that the horsepower represented by the above example is 0.075 horsepower.

It is also of value to note the following identity:

$$2\ \rho\pi R^2 \nu^3 = T\nu \tag{12}$$

The energy to achieve the thrust T must be imparted to the slip stream by the rotor. This energy conversion will not be 100% efficient. It is customary to define

this energy conversion efficiency as --

$$M = \frac{\text{power introduced into slip stream}}{\text{power at the rotor shaft.}} \tag{13}$$

$$= \frac{T\nu}{P} = \frac{1}{\sqrt{2}} \frac{T}{P} \sqrt{\frac{T}{\rho \pi R^2}} \tag{13}$$

An M of .75 is typical of good helicopter rotors. To achieve this value the rotors may have to be tapered and twisted and of full scale.

It may already have been observed that the thrust obtained is proportional to the square of the induced velocity, ν, (equation 9) while the power required to obtain this thrust is proportional to the cube of the induced velocity (equation 11). This argues for rotor designs which call for a relatively low induced velocity, ν, and relatively large volume of air, and is the reason for helicopter rotors being large in diameter.

This relationship may be further understood by the use of the terms "power loading", and "disk loading".

$$\text{Disk Loading, D.L.,} = \frac{W}{\pi R^2} \tag{14}$$

$$\text{Power Loading, P.L.,} = \frac{W}{P} \tag{15}$$

where: W is the gross weight of the helicopter but is equal to T for the hovering case.

Now from equation (13)

$$M = \frac{1}{2} \text{ P. L.} \sqrt{\frac{\text{D. L.}}{\rho}} \tag{14}$$

Assuming sea-level conditions, the above equation reduces to --

$$\text{P. L.} = \frac{38\ M}{\sqrt{\text{D. L.}}} \tag{15}$$

Figure 5 b shows power loading plotted against disk loading for various values of M. Typical disk loadings for large-sized helicopters are in the range of two or three pounds per square foot. For small helicopters such as a microwave-powered helicopter, this disc loading can be a great deal less, resulting in greater power loadings and reducing the size of the motor required.

Another useful relationship which can be derived from the above analysis is:

$$T = 124\ (PRM)^{2/3} (\rho)^{1/3}, \text{ where} \tag{16}$$

T = upward lift, pounds

P = power supplied to rotor, horsepower

R = rotor radius, feet

M = figure of merit

ρ = mass density of air, slugs per cubic foot.

This relationship indicates that the thrust is relatively insensitive to air density. It also indicates that for a fixed rotor diameter, the thrust is proportional to the two-thirds power of the applied shaft horsepower.

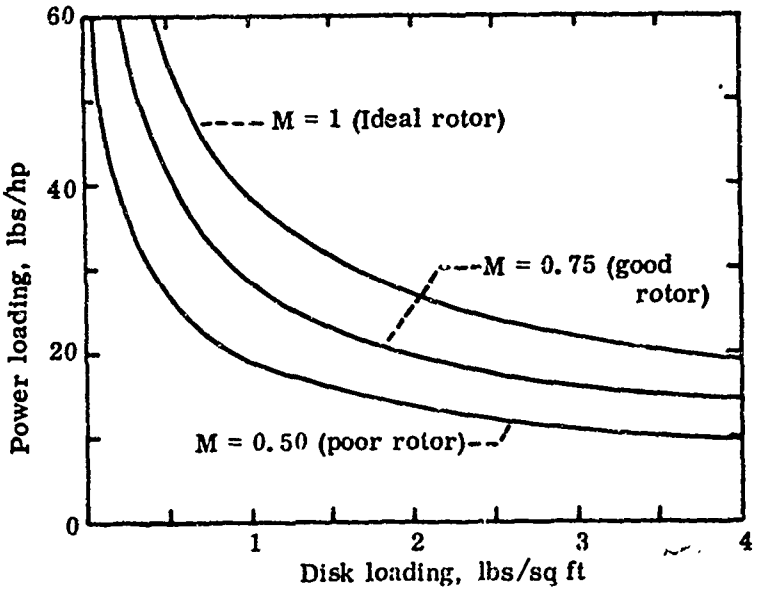

Figure 5(b). Rotor power-loading versus disk-loading curves.

Rotor Blade Construction

The rotors shown in Figure 6 on the microwave-powered helicopter are composed of aluminum, balsa, and mylar. The aluminum and balsa, after assembly and shaping, are impregnated for moisture proofing and covered with a thin film of mylar. Balancing and tracking preceeds flight testing.

The rotors were made by laminating specially selected pieces of balsa of different densities around an aluminum spar of 1/8" x 1/2" cross-section as shown in Figure 7 . The aluminum spar is so placed as to position the chord-wise center of gravity of the blade at or slightly in front of the aerodynamic center of lift lift of the airfoil. A symmetrical airfoil is used so that the shifting of this center of lift with various angle of attack is minute. Higher density balsa is used in the leading edge of the blade to provide both weight and strength. The lightweight balsa used in the relatively flat areas on the top and bottom is 1/3rd the weight of the heavier balsa.

The trailing edge, which tapers down to almost zero thickness, is strengthened by putting the balsa, of which it is composed, into the assembly with its

Figure 6. Top View of Microwave-Powered Helicopter

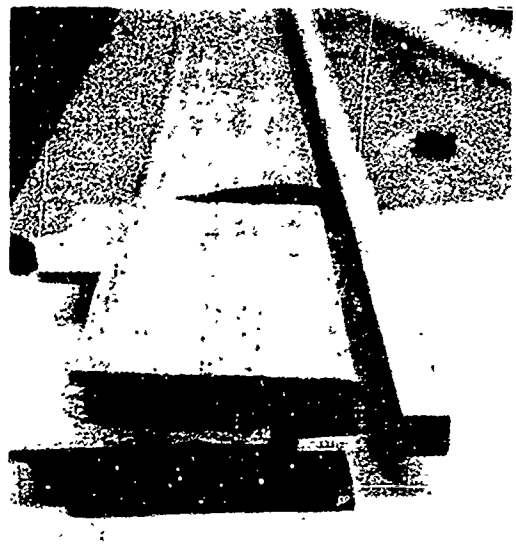

Figure 7. Material Arrangement for Fabrication of the Rotor Blank

grain running across the span rather than along the axis as are the remaining members of the blade. Figure 7 illustrates the manner in which these laminations are positioned.

The laminations are assembled with contact cement. A coating of this material is applied to the pieces of balsa which have first been sealed with clear dope, after which it is allowed to dry 1/2 to 1-1/2 hours. A similar coating of this contact cement without the impregnating layers of dope is applied to the aluminum spar and allowed to dry. The rotors are made in matched pairs. The balsa parts are weighed and matched before final assembly. The parts are accurately positioned individually upon one another with a piece of Kraft paper detween the meeting surfaces. The parts are pressed together as the Kraft paper is gradually pulled out from between the surfaces. Once the two coated surfaces touch one another, the parts cannot be pulled or torn apart without complete destruction of all the wooden members since the bond is appreciably stronger than the balsa members.

Airfoil Generation

The airfoil used is the NACA .0015 of 2.5 inch chord which is normally specified as in Figure 8 and is shown to size in Figure 9. The actual generation of the airfoil from the laminated blank just described is performed on a special machine. A milling machine with a precision high speed spindle was converted so that it could be used for grinding. Grinding leaves a smooth accurate finish after a fast cut and does not bruise the material as other machining approaches might.

The grinding wheel and the machine used to drive it are shown in Figure 10. The machine is a Nichols Miller with a high speed precision spindle. The grinding wheels are placed on the arbor with their axis tilted from the arbor axis a few degrees. This allows the use of several standard wheels rather than one special one.

Station	Upper	Lower
0	0	0
1.25	2.37	-2.37
2.5	3.27	-3.27
5.0	4.44	-4.44
7.5	5.25	-5.25
10	5.85	-5.85
15	6.68	-6.68
20	7.17	-7.17
25	7.43	-7.43
30	7.50	-7.50
40	7.25	-7.25
50	6.62	-6.62
60	5.70	-5.70
70	4.58	-4.58
80	3.28	-3.28
90	1.81	-1.81
95	1.01	-1.01
100	(.16)	(-16)
100	0	0

Leading Edge Radius 2.48

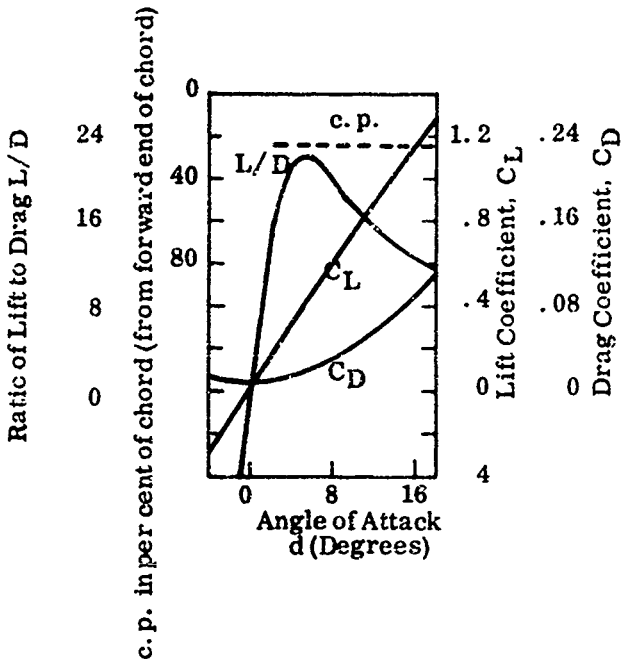

Figure 8. Airfoil Specifications (NACA .0015)

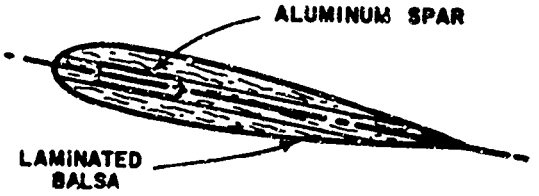

Figure 9. Cross-Section of Airfoil.

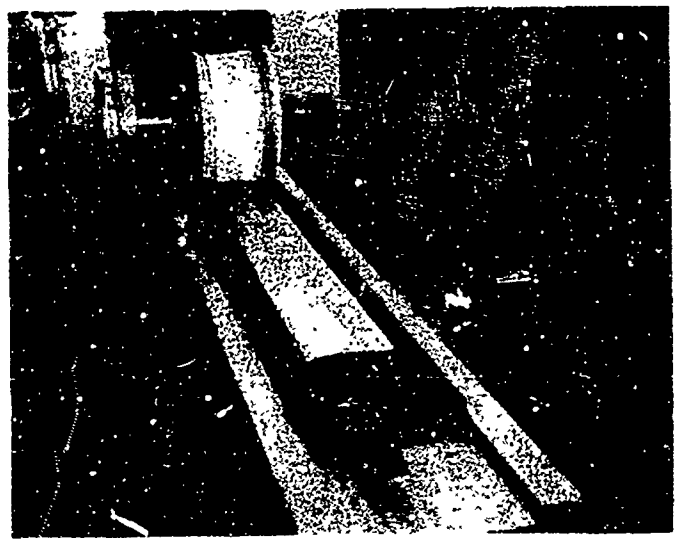

Figure 10. Airfoil Being Shaped on Precision Grinder

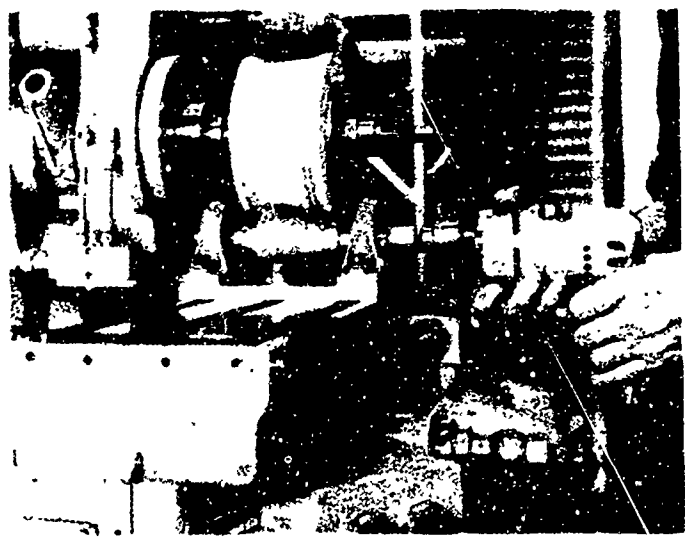

Figure 11. Crush Truing Operation

The blade is fed by hand, in guides which control its position, under the grinding wheel. One pass is required per side.

The shaping of the grinding wheel is performed by a technique known as crush truing. The crush truing feature consists, in this case, of a roll and supporting bearings shown in Figure 11. The roll is made with its outer diameters an accurate replica of the shape the grinding wheel is to reproduce. In use, the fixture is placed directly below the grinding wheel, after which the table of the machine is raised until the truing roll touches the grinding wheel. Next, the roll is driven at a surface speed of 300 feet per minute while the roll is fed upward into the grinding wheel. When the roll touches the grinding wheel, it drives it around and they rotate together. The line-type contact existing between the two cylindrical bodies bearing against each other creates high contact pressure. This pressure, along with the soft wheels used, causes grains of abrasive to break off of the grinding wheel wherever there is contact. This process is continued for 10-15 minutes until the required depth of crushing into the grinding wheel is obtained.

The application of two coats of airplane dope moisture proofs the blades and somewhat hardens and seals the surface.

The covering which is applied after the sealer is dry is a sheet of .002 inch thick clear mylar plastic. This covering serves to increase the blade's ability to withstand light blows and abrasions which would normally dent or scratch the balsa. It also imparts strength to the rotor blade by providing a large strong outside layer which has inherently a high moment of inertia since it is as far from the center line of the member as possible. The mirror-like finish of the mylar has a minimum of aerodynamic drag. This covering is applied with the same contact cement used in the blade fabrication using a similar method of application. Care must be exercised to prevent any wrinkles.

The blades are painted with lacquer and rubbed down for several cycles until a desired finish is obtained and then the blades are ready for mounting, balancing, and tracking.

Balancing and Performance Data

The balancing of the blades on a helicopter is very important. They must have the same mass and their center of gravity both chord-wise and span-wise must be controlled to rather close limits. An important part of this balancing is to "track" the blades, that is, to make both blade tips travel in the same plane.

The control of the chord-wise center of gravity of the blades was not found to be a problem. The weight and the span-wise center of gravity did require some correction. The procedure used was to weigh the blades and measure the distance from one end to their center of gravity, then to add weights such as to make their centers of gravity coincide when their weights were equal.

The attachment used to hold the blades to the rigid rotor hub allows the placing of the two centers of gravity diametrically opposite one another. This same member also contains provisions for varying the angle of attack of the blades.

The tracking of the blades is performed on the test stand shown in Figure 12. The tips of the rotors are observed at their operating RPM with illumination by a stroboscope firing at twice the speed of the blades. The opposite ends of the blades are seen superimposed upon one another. Figure 13 is a multiple exposure of the blade tips out of track. Previously, the blades had had some identifying marks placed on their outside ends. The dynamic position of the blades was changed by increasing or decreasing the angle of attack of one of the blades to respectively raise or lower the tip path plane of that blade so that it "tracked" the other blade.

The test stand mentioned in the previous paragraph was very useful for more than blade tracking. Data were collected on rotor figure of merit, motor efficiency, and lift. Typical data recorded on this setup are displayed in Figure 14. These data were taken with rotor blades 7 and 8 set at a 7^{o} angle of attack.

Figure 12. Static Test Stand for Evaluating Lift and Power Characteristics of Helicopter

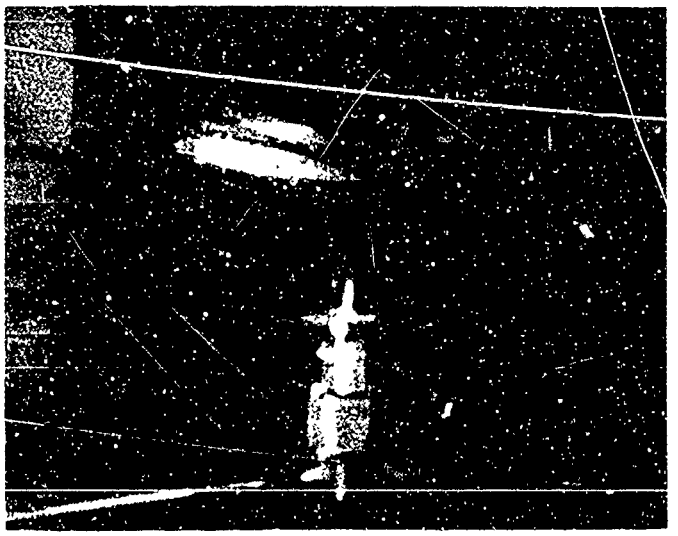

Figure 13. Rotor Tips Illuminated by a Stroboscope Firing at Twice the Speed of the Rotor Blade for Blade Tracking

Lift In Pounds	Reaction Force .573 Ft. Torque Arm	Motor Voltage	Motor Current	Rotor RPM
3.5	1-5/8	81.0	1.59	332
4	1-3/4	86.2	1.68	347
4.5	2-1/16	91.8	1.70	373
5	2-3/8	98.0	1.75	387
5.5	2-1/2	103.1	1.80	402
6	2-11/16	109.2	1.91	421
7	3-3/16	131.0	2.15	456
7.5	3-7/16	135.3	2.22	466
7.75	3-1/2	138.8	2.28	481

Figure 14. Rotor Performance Data for Blades 7 & 8 with Angle of Attack set for 7^{o}.

The motor's voltage and current for a particular value of lift were recorded. The lift was determined by substracing the weight at a particular operating level from the known static weight observed before the test run began. Weight was added to the system until it weighed 12 pounds.

Next, the blade rotation speed was measured with a stroboscope, after which the reaction torque of the driving motor was measured and recorded. This could be measured since the motor was mounted on top of a shaft which was free in ball bearings both to move up and down and to rotate with a very minimum of friction.

The aforementioned data were reduced to a more easily evaluated parameter as in Figure 15. The column titled "watts input" was converted to horsepower input by the factor 746 watts/hp. The horsepower input, in turn, was compared with the horsepower output to obtain the over-all efficiency of the motor gear housing assembly. The calculations performed to determine the horsepower input to the rotor used the relation $HP = \frac{2\pi (RPM)\ (TORQUE)}{33,000}$ where the torque of the motor is the force which drives the rotor. This torque is the force measured tangential to a disc mounted on the motor support shaft times its moment arm, the radius of the disc.

The next to last column of Figure 15 is the pounds of lift divided by the horsepower consumed by the rotor. These data, along with the last column, the pounds of lift divided by the area of the rotor, are used to determine a rotor's figure of merit and are presented in Figure 16. The solid lines are for rotor figure of merit. Unity is the ideal figure of merit with cases of M = .75 and M = .50 for good and poor rotors, respectively. A so-called good rotor is invariably one having twisted tapered blades. It was considered unnecessary and undesirable economically to become involved with twisted tapered blades during this program.

A more useful and informative manner to look at the rotor blades for this work is to plot lift in pounds as a function of motor output horsepower. Figure 17 shows these data for rotor angles of attack of 5°, 7°, and 9°.

Lift in Pounds	Watts Input	Horse-power Input	RPS	Torque Foot Pounds	Horse-power Output	Motor Trans-mission Efficiency	Power Loading, Pounds Lifted Per Horsepower Consumed By Rotor	Disc Loading, Pounds Lifted Per Sq. Ft. Of Area Swept By Rotor
3.5	128.0	.173	5.54	..932	.0587	33.9	59.3	.1105
4	143.0	.193	5.78	1.003	.0667	34.5	60.0	.1264
4.5	154.4	.207	6.22	1.181	.0835	40.0	53.8	.1240
5	171.0	.2283	6.45	1.360	.1003	44.4	50.0	.1678
5.5	186.0	.249	6.70	1.435	.108	43.4	50.9	.1735
6	208.0	.278	7.02	1.540	.1262	45.3	47.6	.1894
7	282.0	.378	7.61	1.825	.1565	41.4	44.7	.2205
7.5	298.0	.399	7.76	1.970	.1745	43.7	43.0	.2364
7.75	318.0	.426	8.02	2.002	.1830	42.9	42.3	.2524

Figure 15. Evaluation of Data in Figure 14 in Terms Applied to Motors and Rotors.

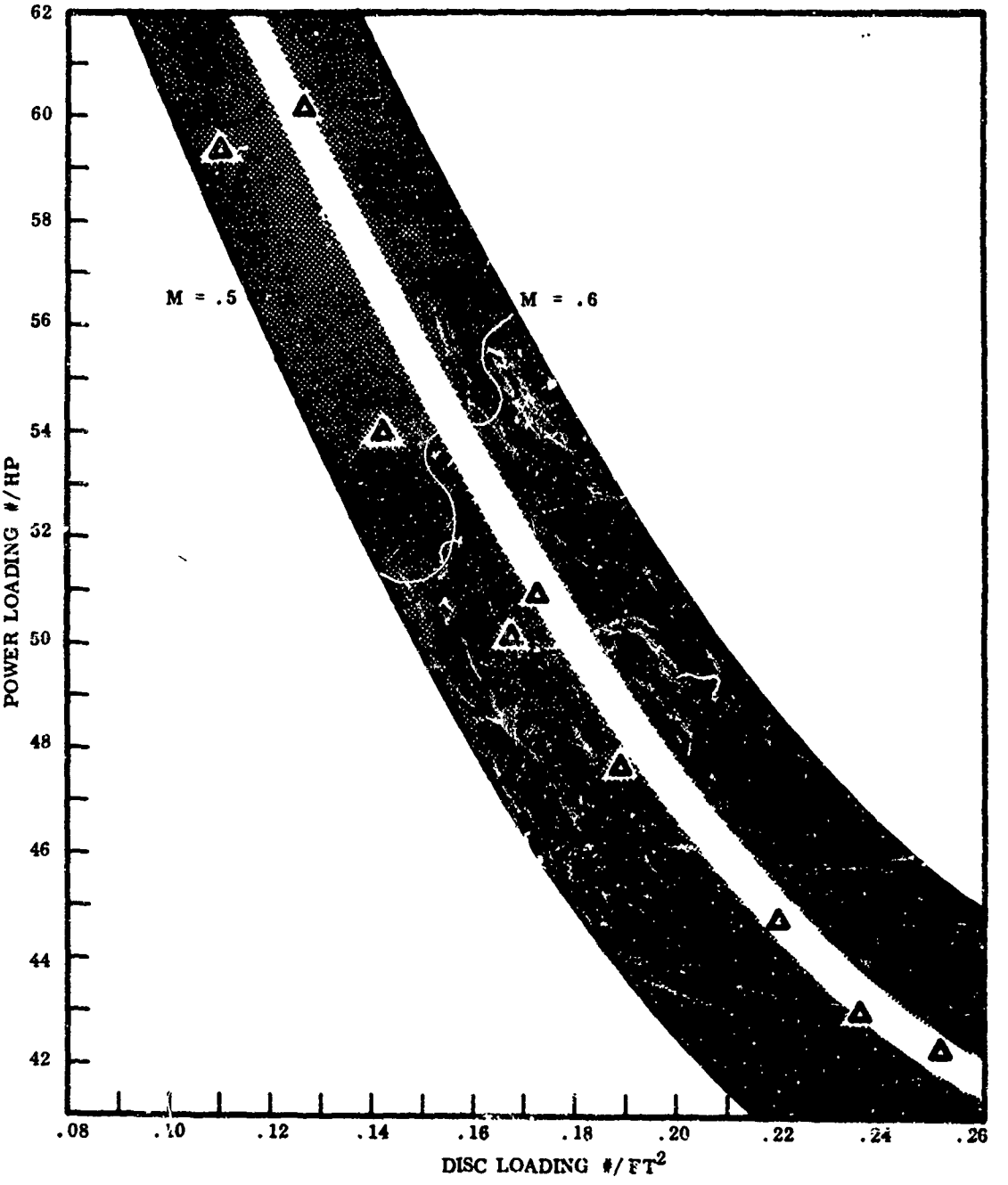

Figure 16. Plot of Last Two Columns in Figure 15 Showing Figure of Merit for Rotor Blades 7 & 8 with an Angle of Attack at 7°.

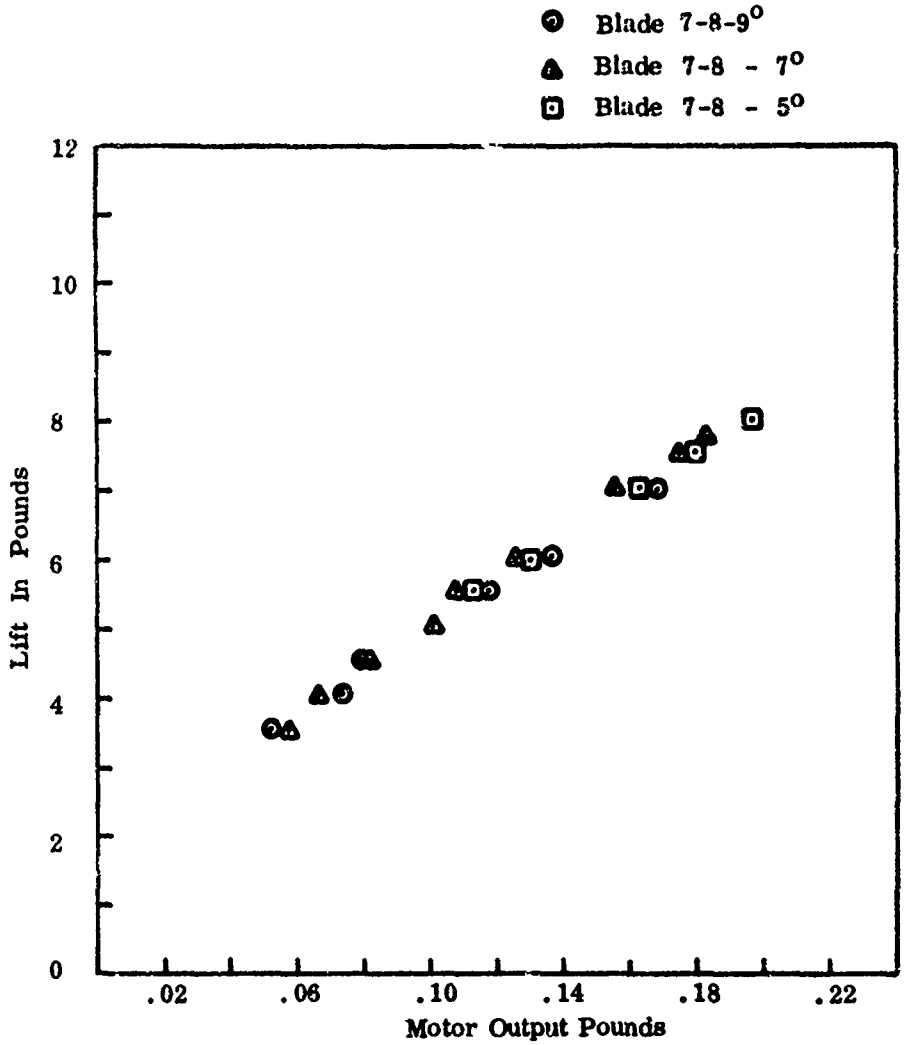

Figure 17. Lift in Pounds Generated by the Rotor as a Function of the Power Consumed by the Rotor for Blades 7 & 8 with an Angle of Attack at 5, 7, & 9 Degrees.

The weight of the craft we were flying varied between 4.5 and 5.5 pounds. The craft used during the ten hour outside flight weighed 5-1/4 pounds and when it was just hovering consumed about 200 watts which was delivered to it from the rectenna. However, we kept the craft pushing upward against a weight, so it was actually consuming considerably more than 200 watts.

Several subtle trade-offs are involved when deciding the angle of attack that the rotor will be set at. If the flight is to be in a calm area, then wind effect can be disregarded and the blades can be set for maximum lift with minimum power consumed. On the other hand, should the flight be outside, then one must consider wind effect. Here, the angle of attack can be lowered, resulting in higher blade speed and better performance.

Wind Effect

Initially, operating outside in the presence of winds of 10-15 MPH presented problems. The craft was subjected to vibrations while losing considerable lift. The three factors contributing to this were:

1. Differential Lift. This occurred when the blade advancing into the wind experienced an increased velocity with respect to the wind, resulting in increased lift, while the rotating blade going downwind responded to a lower resultant wind velocity and lift. The effect was to roll the craft. The center tether restrained and straightened the craft to a vertical altitude as the blade rotated through the region where this occurred. The net effect was a two per revolution rolling moment vibration.

2. Blade Stall. The stall of a wing limits its low speed. When the speed relative to the wind of the rotating blade slowed down to a point where the blade started to stall, the drag was appreciable while the lift fell off drastically.

3. Tether Wire Resonances. Vibration in the craft can be amplified by the tether wires.

The removal of the rolling movement resulting from the differential lift could be accomplished by:

(a) installing flapping and lagging hinges where the rotor joined the rotor hub.

(b) cyclically changing the attack angle or pitch of the rotor blades as they travel around the hub.

(c) tilting the rotor axis into the wind so that the advancing blade had effectually a lower angle of attack while the rotating blade had an increased angle of attack.

Reasons of expediency caused us to employ the flapping and lagging hinges first. This assembly, shown in Figure 18 in two views, allowed the blades to rise when they experienced additional lift without exerting any movement about the rotor hub. The lagging hinge is required to allow the blade to maintain a relatively constant momentum. When the blade flaps up, its center of gravity is drawn closer to the center line of rotation. The lagging hinge allows the blade to coast forward during this period and to lag behind when less lift is experienced and the blades flap down. Tests in windy conditions confirmed the action of these hinges. They did indeed reduce the rolling movement. However, a new problem appeared when the blades at low RPM tended to oscillate on the lagging hinges. The center of gravity of the rotor was rapidly shifted appreciably from one side of the craft to the other and the interaction of this shift and the resulting development of the craft springing out of position in the tether wire system twice nearly destroyed the craft.

This problem is experienced on all helicopters employing the flap and lag hinges. They run into it most frequently when a pilot allows his craft, during a landing, to hit on one skid causing the craft to roll quickly about that skid. When this happens,

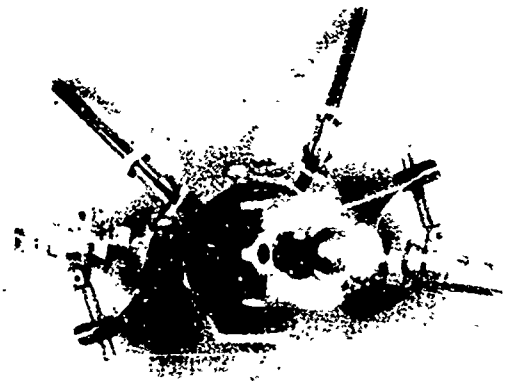

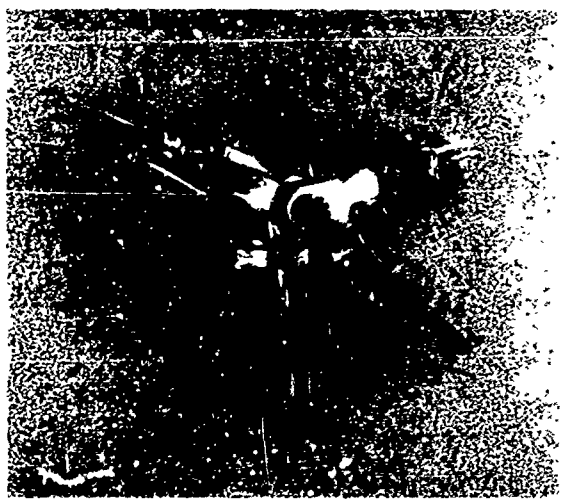

Figure 18. Rotor Hub with Flapping and Lagging Hinges

the rotor's center of gravity experiences a sudden shift in the opposite direction relative to the craft. The landing of the second skid on the ground frequently about a half cycle later accomplishes this condition. This can and does quickly destroy the craft if immediate action to apply a substantial amount of power to the rotor is not taken. The term applied to this phenomenon is "ground resonance." Partial control can be obtained by the use of "drag linkage" or "dampers" which damp out the oscillation.

Concurrently, while working and testing the flapping and lagging hinges, we built a gimbaled rotor hub assembly which also contained flap and lag hinges. The thinking that brought this about arose from consideration and evaluation of the second and third causes of vibration in the outside flight during high winds, stalling the blades and tether vibrations. Professor Ham of MIT, a consultant to Raytheon in matters concerning helicopter design, calculated the region of stall of rotors with 0^{o} of tilt into the wind and with 10^{o} of tilt for 0.1, 0.2, and 0.3 shaft horsepower. These data are plotted as a function of the lift generated by the rotor in Figure 19. These curves show an increase in thrust or lift with increasing wind velocity. Although we have not been able to identify this phenomenon, most likely it occurs because the regions of stall occur earlier than indicated. Also, stall is not cleancut, but a mushy thing with no sharp boundary. The conclusions which can be drawn from this thinking are:

(a) stall is a low speed problem, so lowering the angle of attack of the blades will manifest itself in an increased rotor speed which helps appreciably to decrease the amount of stall.

(b) tilt the rotor with a gimbal to increase lift and to raise the wind velocity at which stall will occur on the rotating blade.

(c) the tilting of the rotor axis into the wind reduces the angle of attack of the advancing blade and increases the angle of attack of the retreating blade. This decreased the lift of the advancing blade and increased the lift of the retreating blade which minimized the differential lift and resulting rolling movement vibration experienced earlier.

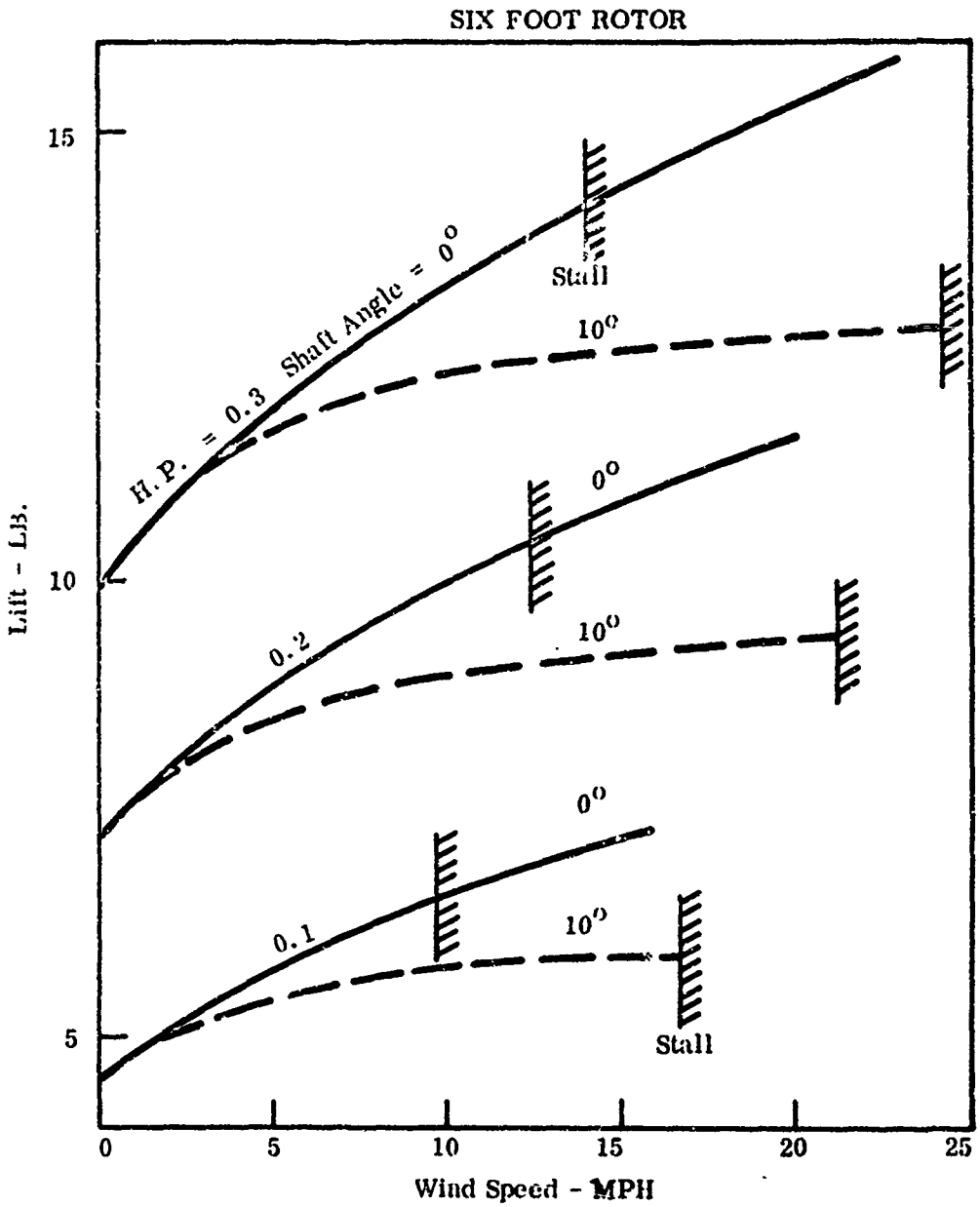

Figure 19. Lift versus Wind Speed Showing Regions of Stall with Rotor Axis Vertical and Tilted Into the Wind 10°. Values for 0.1, 0.2, and 0.3 Horsepower are Shown.

The gimbal which was used to tilt the rotor into the wind is shown in two views. Figure 20 was taken from the driven end of the assembly. The members to which the rotor blades themselves attach project out to the right and left. Projecting counterclockwise off these lagging hinged members are the drag linkages. The control rods which are used to tilt the rotor in any direction up to 20° from the vertical are pointing upward in this view. They are attached to the rotating gimbal through joints and a large thin ball bearing.

The lower view, Figure 21 shows a side view of the gimbaled rotor hub. One of the rotor mounting members projects to the right side of the picture and the other one in a position of extreme flapping action projects upwards from the left side. The control rods are pointing to the lower right. This structure contains four ball bearings in the gimbal itself, one ball bearing for joining the control mechanism to the gimbal, one ball bearing to allow the wire riding mechanism inside the assembly to turn on the wire, and three more ball bearings to ride on the wire.

The weight of the gimbaled rotor hub assembly complete with flap and lag hinges and drag links is 0.42 pounds. The rotor blades themselves weigh 0.85 pounds.

The system was tested out of doors on October 16, 1964 while the wind was varying between 10 and 15 miles per hour, northwesterly. The test ran for some time with very little vibration and everything looked good. The rotor was pitched into the wind 7°. Trouble developed however when we brought the craft down for a landing. The same ground resonance which had previously bothered us when we had no drag links occurred again. The effect was rather drastic and the craft as well as the wires were severely shaken. The torque resisting arms came out of the terminals and the end of one rotor blade smashed into one of the outside vertical tether wires. The tip of this rotor was traveling something less than the normal speed of 90 MPH as the rotor was

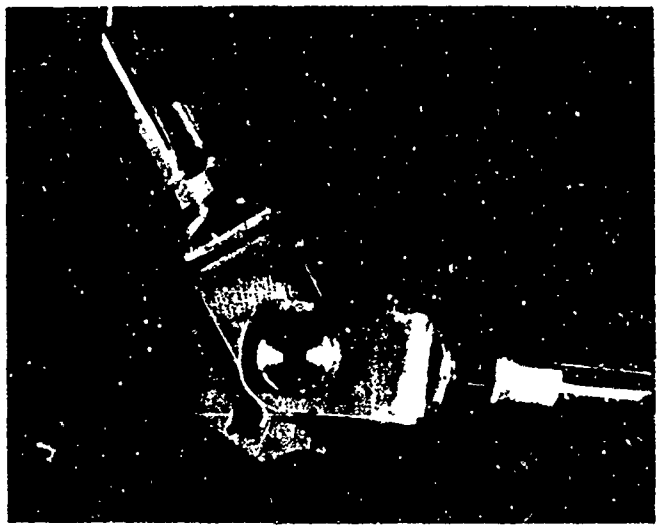

Figure 20. View of Gimbaled Rotor Assembly from Driven End

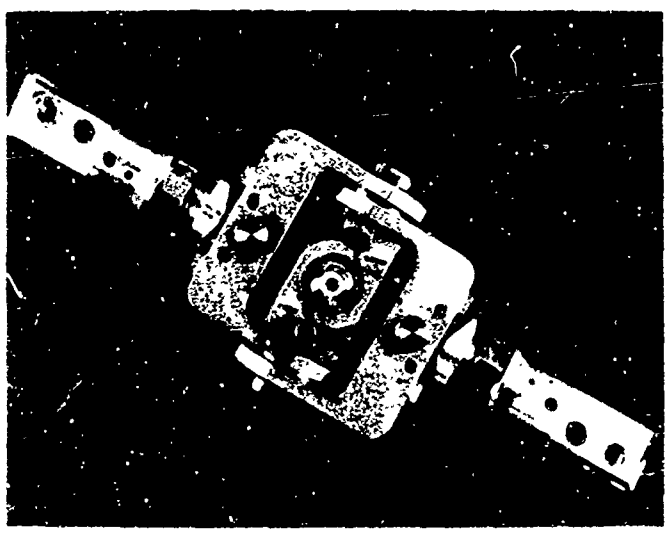

Figure 21. Side View of Flapping and Lagging Hinge Assemblies with Drag Linkages Incorporated Into the Gimbaled Rotor Hub

slowing down. Nonetheless, it still contained considerable energy when it hit the wire. The blade suffered no real harm other than a dent about 1/8" deep in the leading edge and 3 or 4 chord wire stretch marks in the mylar covering. These blades have seen a lot of use since then and are still quite usable. This problem was overcome by rigidly attaching the rotor blades to the gimbaled rotor hub. No problems of this nature have reappeared since.

High Winds

Flights were successfully accomplished in winds of up to 25 MPH by using the gimbaled rotor hub with a 7° angle of attack rotor setting. The rotors were rigidly attached to the rotor gimbal hub. Various effects were created when the wind was from different quarters. As might be expected, a wind from the north which came over the building made flight difficult. This is due to the downdraft created. On the other hand, a wind from the south tended to lift the craft up and made flight possible with appreciably less power. Winds from the east and west created vibration problems at first, but these were eliminated so that no real problem prevailed as long as the winds were less than 20 MPH and the rotor was tilted in the correct direction for approximating the correct amount.

3.2 MOTOR AND GEAR HOUSING

The motor gear housing assembly takes the electrical output of the rectenna and transforms it into appropriate mechanical motion suitable to drive the rotor blades. While performing this function efficiently, it must also be lightweight, be adequately rigid mechanically, and provide a means to join some members of the craft together. The method of tethering we employed also required that the motor gear housing assembly have a clearance hole axially through its center.

The armature, field winding and brush holding assemblies were parts obtained from a 1/4" electric hand drill purchased at a local hardware store. New lower ball bearing mounts for the armature, which also provided tether arm mounting, were attached to the lower end of the brush holding assembly and a new gear housing was attached to the upper portion of the brush holding assembly. Figure 22 is a photograph of these parts disassembled. A hole has been drilled through the center of the armature. The ability to put this hole through the armature along with a gear housing design having a concentric output shaft made it relatively easy for us to shift to the center tether method of guidance.

Figure 23 is a photograph of the top of this transmission assembly with the top and intermediate bearing support plate removed enabling the gears' position to be observed. The position of the armature under this transmission can be determined by the ends of the cooling fan projecting out from under the lower portion of the transmission.

The weight of the motor system without the transmission and its gears is 1.42 pounds and the armature comprises 35% of this. The weight of the transmission with its bearing and gears is 0.67 pound and this brings the total weight of the motor transmission assembly to 2.1 pounds.

The transmission consists of bearings, gears, and housings to contain and align these members. The output of the transmission is coaxial with the input

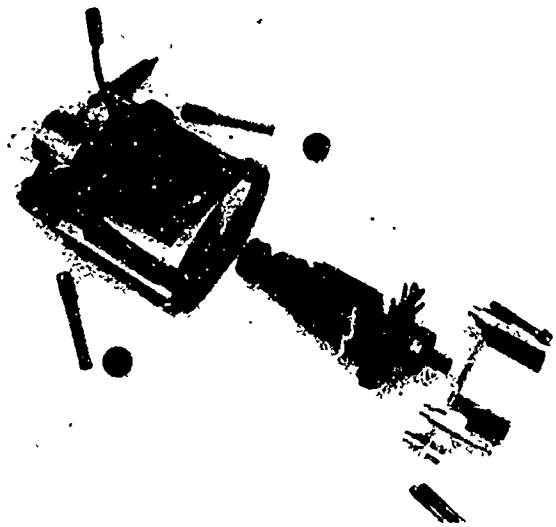

Figure 22. Exploded View of Motor Assembly

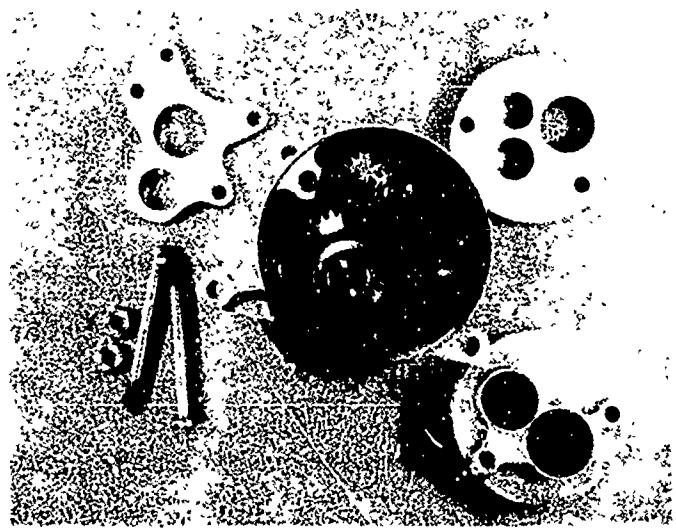

Figure 23. Top View of Transmission with Bearing Support Plates Removed to Show Gear Positions

and closely adjacent to it. Between the input pinnion and the output gear are four other gears, two on each of the two shafts, which together reduce the 16,000 rpm of the armature down to the 400 rpm of the rotor blade. Figure 24 shows how the gears mesh and provides a tabulation of the pertinent dimensions of these gears and the forces acting on the teeth of the gears while transmitting 1/2 horsepower to the rotor.

These gears as well as the armature of the motor were all mounted on class 5 to 7 precision ball bearings with presealed lubrication. The transmission housings were machined to precise dimensions and the gears then shaved to fit. The hardness of the gears was individually tailored to the particular job that gear performed. The pinnions are 38-40 rockwell, and the gears are 32-34 rockwell.

It can be seen from this table of gear sizes that the total gear reduction is 40 to 1. Provisions were made in the design of this transmission to allow this ratio to be changed by replacing the last two gears in the chain with ones either slightly larger or smaller in size by one tooth. One tooth would not be expected to make a large difference, but the change is made on two gears at one time and it is on the end of a gear train so it is larger than might be expected at first glance. Changing these last gears changes the 40 to 1 ratio to 36.6 to 1, or to 43.2 to 1. This permits considerable control on the motor's voltage and current or armature speed.

Data on the ball bearings used in the motor and transmission are listed in Figure 25, the letters referring to the position of each bearing in the motor transmission assembly. The loads shown acting on these bearings are for a load of 0.5 horsepower which is considerably higher than we required.

The over-all efficiency of the motor gear transmission was a nominal 45%. Figure 26 is a plot of some of the data on efficiency as a function of the output horsepower of the motor for attack angles of 7^{o} and 9^{o}.

GEARING DESIGN PARAMETERS - 20° PRESSURE ANGLE

Gear	No. of Teeth	Diametrical Pitch	Pitch Dia.	Loaded Speed	Pitch Line Velocity (ft/min)	Torque Transmitted (in/lbs)	Reduction Ratio	Force Acting on Tooth Face (lbs)	Separating Force (lbs)
A	9	40	.224	18,750	1,100	.84		11.1	1.79
							4.89		
B	44	40	1.100	3,830	1,100	4.11		11.1	1.79
C	11	32	.345	3,830	345	4.11		33.7	8.7
							3.27		
D	36	32	1.125	1,170	345	13.45		33.7	8.7
E	16	32	.500	1,170	153.5	13.45		76.0	19.6
							2.5		
F	40	32	1.250	468	153.5	33.6		76.0	19.6

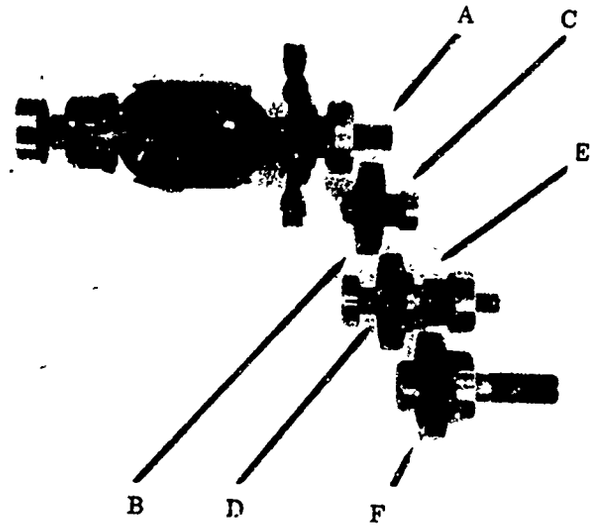

Figure 24. A Tabulation of the Transmission's Gear Design Parameter and a View Showing Each Gear's Position in the Train

TRANSMISSION BALL BEARING DATA

Design Life 3800 hrs at 5 times the Operating Horsepower

Bearing Train #	Bearing Identification #	OD/ID	Operating Speed RPM	Radial Load Capacity at Operating Speed lbs	Calculated Gearing Load to be Applied to Bearings
A	SR6FF	.875/.375	18750	45	1
B	SR6FF	.875/.375	18750	45	4
C	SR2FF	.375/.125	3830	14	4
D	SR3FF	.500/.1875	3830	28.5	20
E	SR4FF	.625/.250	1170	46	44
F	SR4AFF	.750/.250	1170	79	70
G	SR4FF	.625/.250	468	46	40
H	SR6FF	.875/.375	468	146	40

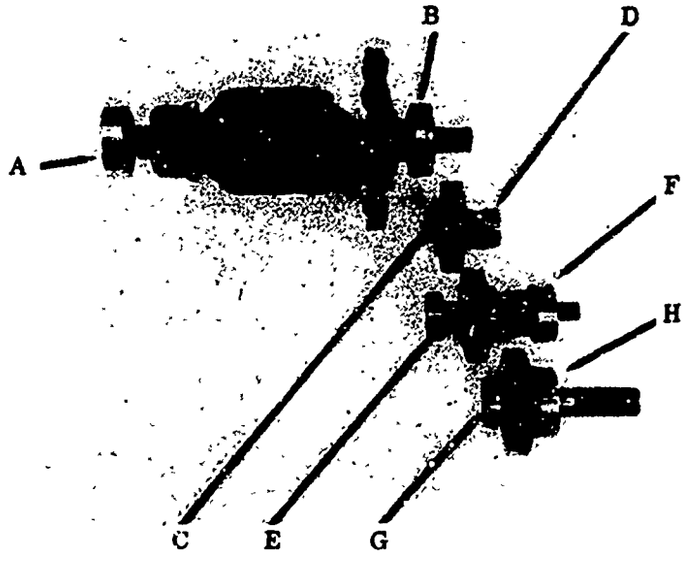

Figure 25. A Tabulation of the Transmission's Ball Bearing Load Data and a View Showing Each Ball Bearing Position in the Train.

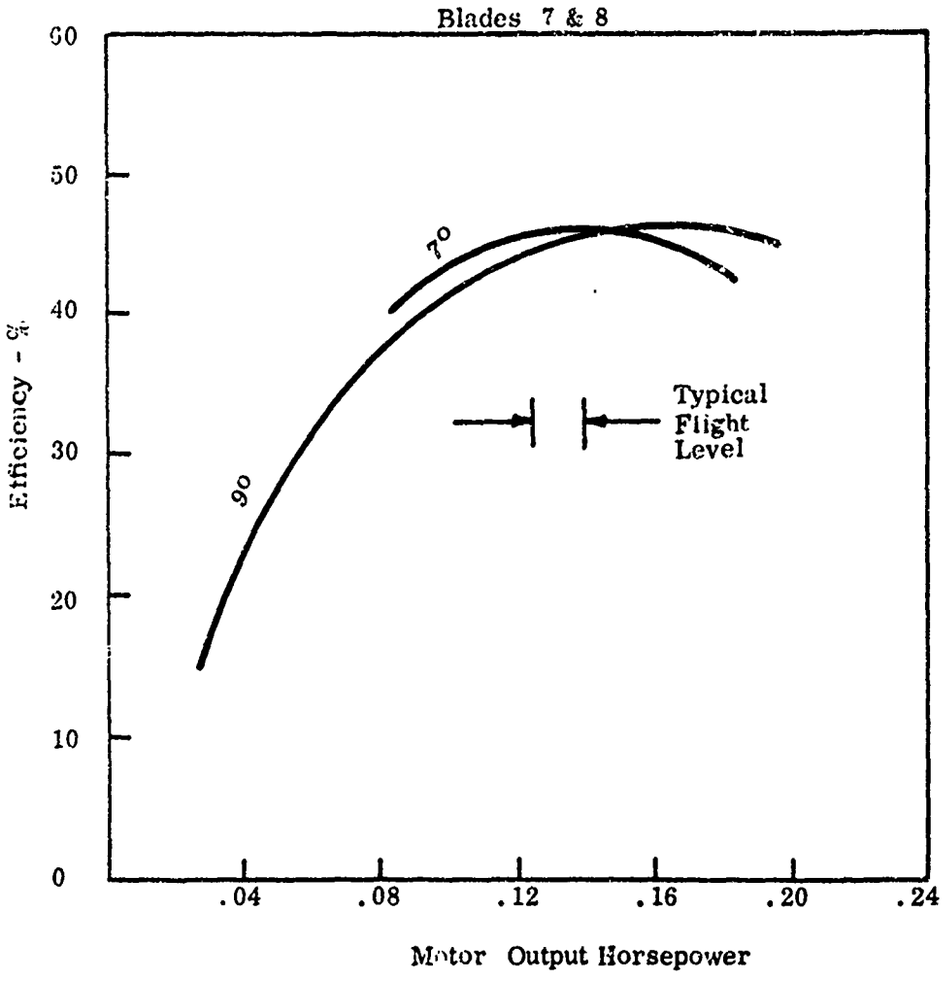

Figure 26. Over-All Efficiency of Motor Transmission Assembly.

3.3 TETHERS

Tethers are used to keep the helicopter confined in all degrees of freedom excluding the vertical. The tethering system is shown in Figure 2. The building is the Super Power wing of Raytheon's Spencer Laboratory -- the view looks north. The boom of 1000 pound capacity projects out from the tope of the cupola 10 feet and is 12 feet above the 50 foot high roof of the cupola. This boom is held in position over the transmitting dish below by a removable index pin.

Hanging down from the boom are three tether wires. The two outside wires are 1/8" diameter stainless steel and go vertically downward to be attached under tension to the foundation which also supports the 9.7 foot diameter transmitting dish. These wires are stretched 3/4 of an inch placing them under a 50,000 PSI stress. The yield strength of this material is in excess of 100,000 PSI. Projecting outward from the craft are two torque resisting arms which contact these wires through ball bearings controlling the craft's rotation. Figure 27 shows the relative position of these three tether wires to the boom and to the microwave-powered helicopter.

The center wire tether which is .078 inch diameter stainless steel is also stretched 3/4 of an inch. This wire goes from the center of the upper terminals of the two outside wires downward through the rotor hub, gear transmission, motor armature, and the rectenna to be attached to a quick acting clamp mounted upon a waveguide bend which is part of the rf-feed to the transmitting reflector. This bend as well as the reflecting dish are rigidly bolted to members which are attached to concrete footings as shown in Figure 28. The center wire constrains the craft in lateral degrees of freedom as well as in roll and pitch. Figure 4 shows the craft installed on the wire and being checked to determine if there is any binding.

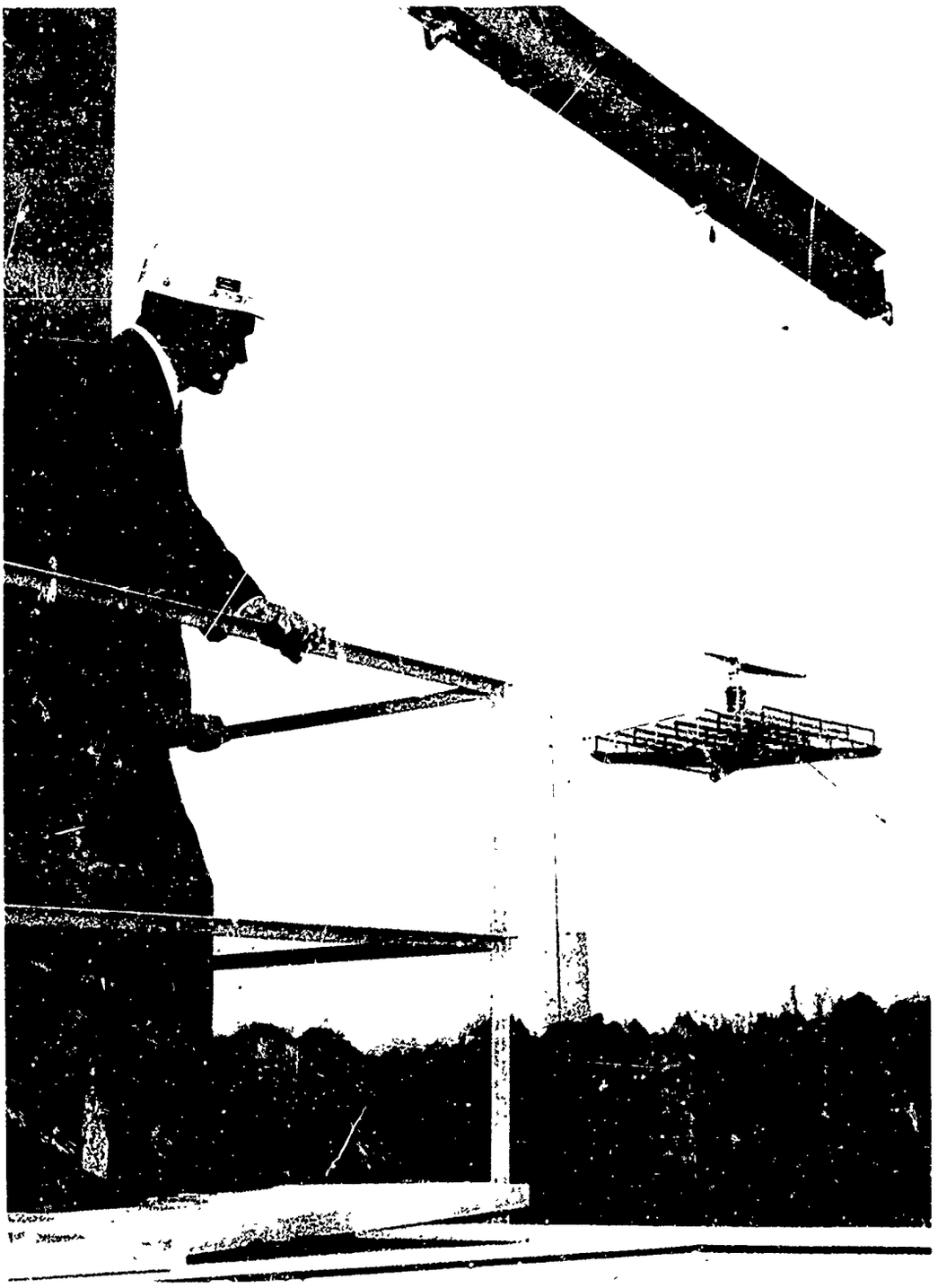

Figure 27. View of Helicopter in Flight Near Top of Tethers Showing Relative Positioned Tethers, Craft, and Boom

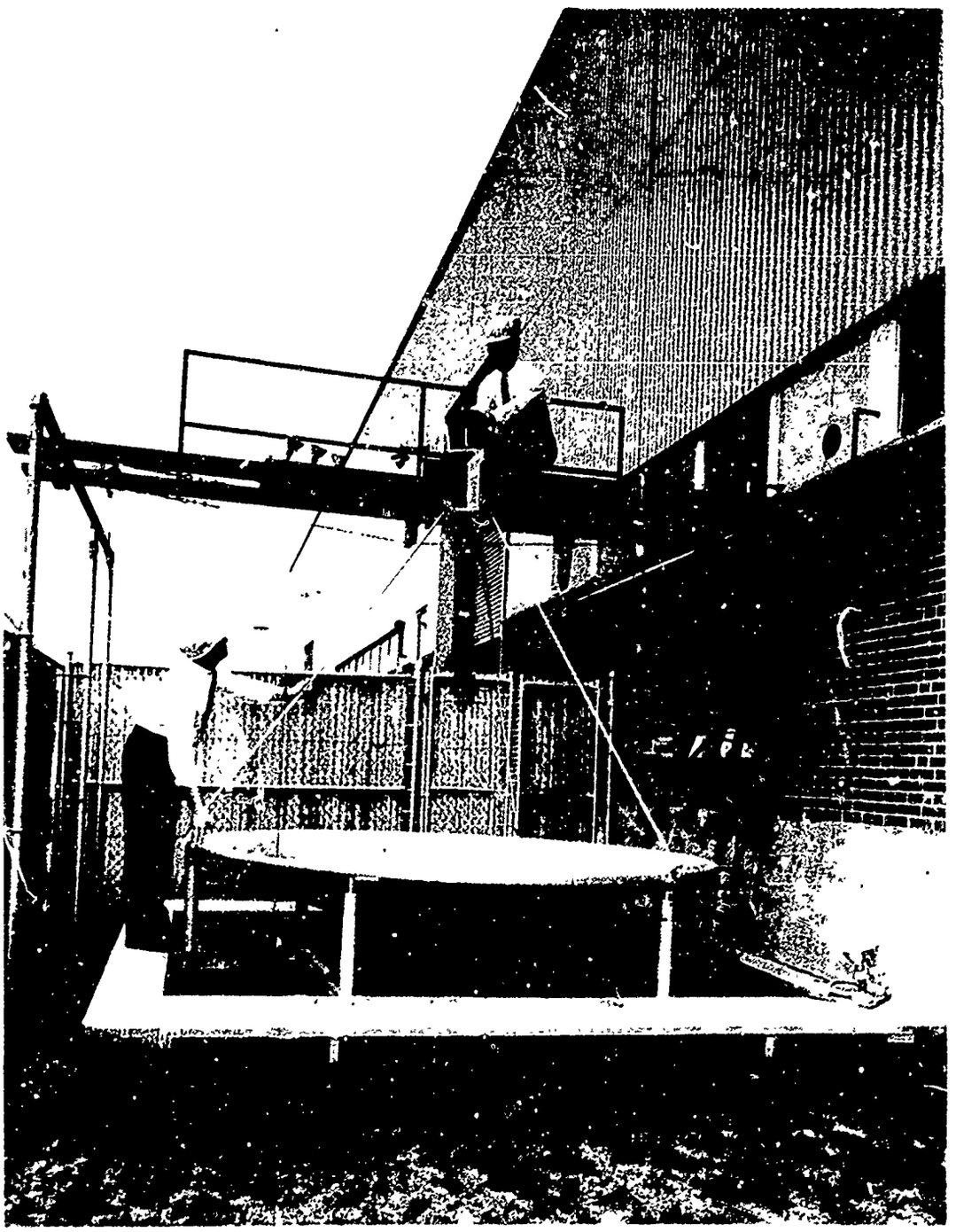

Figure 28. Reflecting Dish and Feed Horn Assembly Rigidly Mounted to Steel Beams which are Bolted to Concrete Footings

Running up and down on the center wire as well as the outside wire is a carrier. This unit is used to lift the craft up to the level where we wish the flight to begin. Typically, this level was about 30 feet although flight could be begun as low as 18 - 20 feet. The carrier was raised and lowered on dacron lines which went up to the boom and then over to the building and down to a salt-water, level-winding fishing reel. A second reel was used to control a line used to raise and lower models on the center tether during experimentation. This same line was also used during the 10-hour flight to hold a one pound weight 52 feet above the face of the dish. This weight served to prevent the helicopter from climbing to an altitude higher than 52 feet.

The preceding discussion pertained to the outside setup and its tethers. An additional testing range had been previously set up and used indoors. This testing setup consisted of a dish, like the one used outside, held on its edge so as to project the beam of energy parallel to the floor. Thirty-two feet from the face of this dish a 4' x 4' x 45^{o} aluminum reflector directed the beam vertically upward. An arrangement similar to the tether outside was used here, differing mainly in that it was shorter in height. Figure 29 shows the craft on the wire and ready for flight.

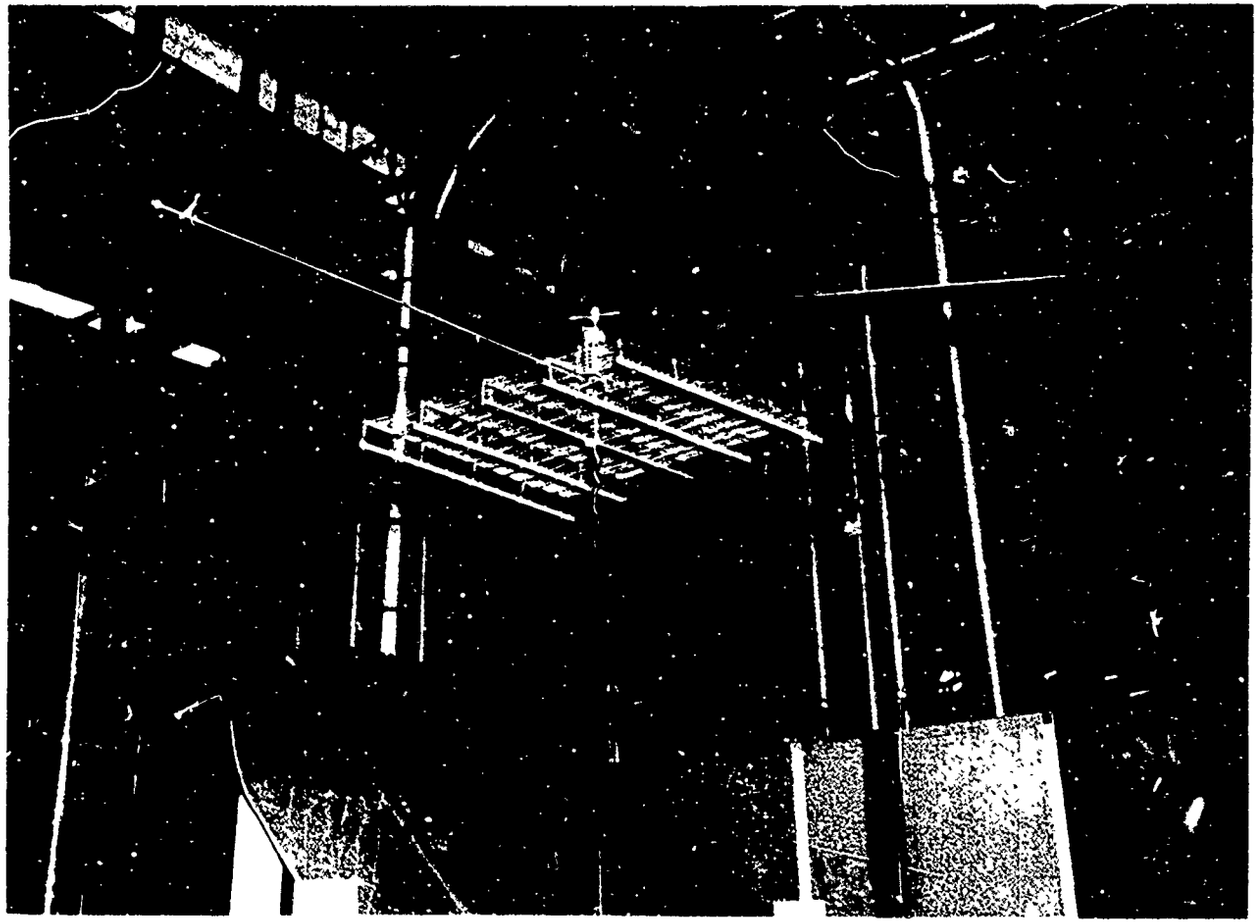

Figure 29. The Microwave-Powered Helicopter Installed at the Inside Flight Testing Range. The 45° Reflector Used to Deflect the Beam to the Vertical can be Seen Below the Craft

3.4 THE COMBINATION RECEIVING ANTENNA AND RECTIFIER

The key to a successful application of the transmission of microwave power to aerospace vehicles lies in the interception and rectification of microwave energy with devices that have a high ratio of power handling capability to their weight, are reasonably efficient, and can be cooled easily without adding weight or other complication. An additional practical need is for the capture antenna to have nondirectional characteristics in order to dispense with weight problems concerned with maintaining dimensional tolerances and proper pointing of a directional antenna.

The first approach to the solution of this problem was the concept of breaking up the receiving aperture into a number of smaller horns or parabolic reflectors, each terminated with an efficient rectifier of sizeable power handling capability. Such a concept still left considerable directivity in the array and introduced a problem of disposing of the dissipated power in the rectifier. Neither one of these problems is a severe one with land-based installations, but both of them represent severe problems in an aerospace environment. Nevertheless, the first attempts to fly a microwave-powered vehicle were made with this approach and the practical difficulties encountered emphasized the superiority of a different approach not as far advanced but with the inherent capability of providing all of the requirements of an aerospace receiving antenna and rectifier.

The basis for the new approach was an outgrowth of work on the use of the point contact silicon semidonductor diode at Purdue University. In this program of work it was determined that the silicon point-contact diode made an efficient rectifier but that its power handling capability was so low that it would require twenty thousand diodes, representing a weight of four pounds without any supporting structure included, to supply a kilowatt of power. This was entirely too much weight for the longer range objectives of microwave-powered helicopters, but there was substantial hope that the ratio of power handling capability to weight could be improved by a diode development program.

The development which precipitated serious consideration of the use of the semiconductor diode for an airborne vehicle was the determination by a Raytheon-

sponsored program that the diode could be successfully incorporated into an antenna array consisting of half-wavelength dipoles spaced a half-wavelength from each other, a quarter-wavelength in front of a metallic reflector, and each terminated by four diodes in a bridge-rectifier configuration as shown in Fig. 30. Such an array was found to have somewhat better directivity than a single-half-wave dipole, as shown in Fig. 31, and the combined capture and rectification efficiency of such an assembly was found to be close to 50%.

While a combination antenna rectifier of the half-wave dipole configuration should have some direct application, the power-handling capability of such an array using the diodes then available was only five watts per square foot which was entirely too small for an experimental microwave-powered helicopter. Attention was therefore directed to packing many more diodes into a given area, leading to the arrangement of bridge rectifiers shown in Figure 32, and the general concept of the diodes representing an admittance sheet in space. The construction of a typical six-inch square module of 280 diodes which gave a power output in excess of 14 watts when inserted in the antenna is shown in Figure 33.

The semiconductor diodes used were type number 1N82G. These were made by New Japan Radio Co., Ltd. and were selected because of their combination of satisfactory performance qualities and low cost. In performance and package size they were similar to the Sylvania 1N830 which had been successfully used in the earlier Purdue investigations of semiconductor diodes used as microwave rectifiers.

The admittance sheets represented by these strings of diodes are not well matched to space, however, nor are they self-supporting in a large antenna array. The conductance represented by these sheets is about ten times that of space, so an inordinately large amount of power is reflected from them. On the other hand, very little power is transmitted through such an admittance sheet.

Fortunately, a solution was found to both the matching problem and the mechanical support problem by placing a grating consisting of a plane of parallel rods in front of the plane of diodes and adjusting it to achieve a maximum saturable power output from the diodes. Spacers placed between the rods and the diode modules provided support for the plane of diodes. As a result of this program, the total weight of the two-foot square 4480 diode, self-supporting antenna array with an operating level of 250 watts was just slightly over two pounds, representing a specific combined weight of antenna and rectifier of eight pounds per kilowatt.

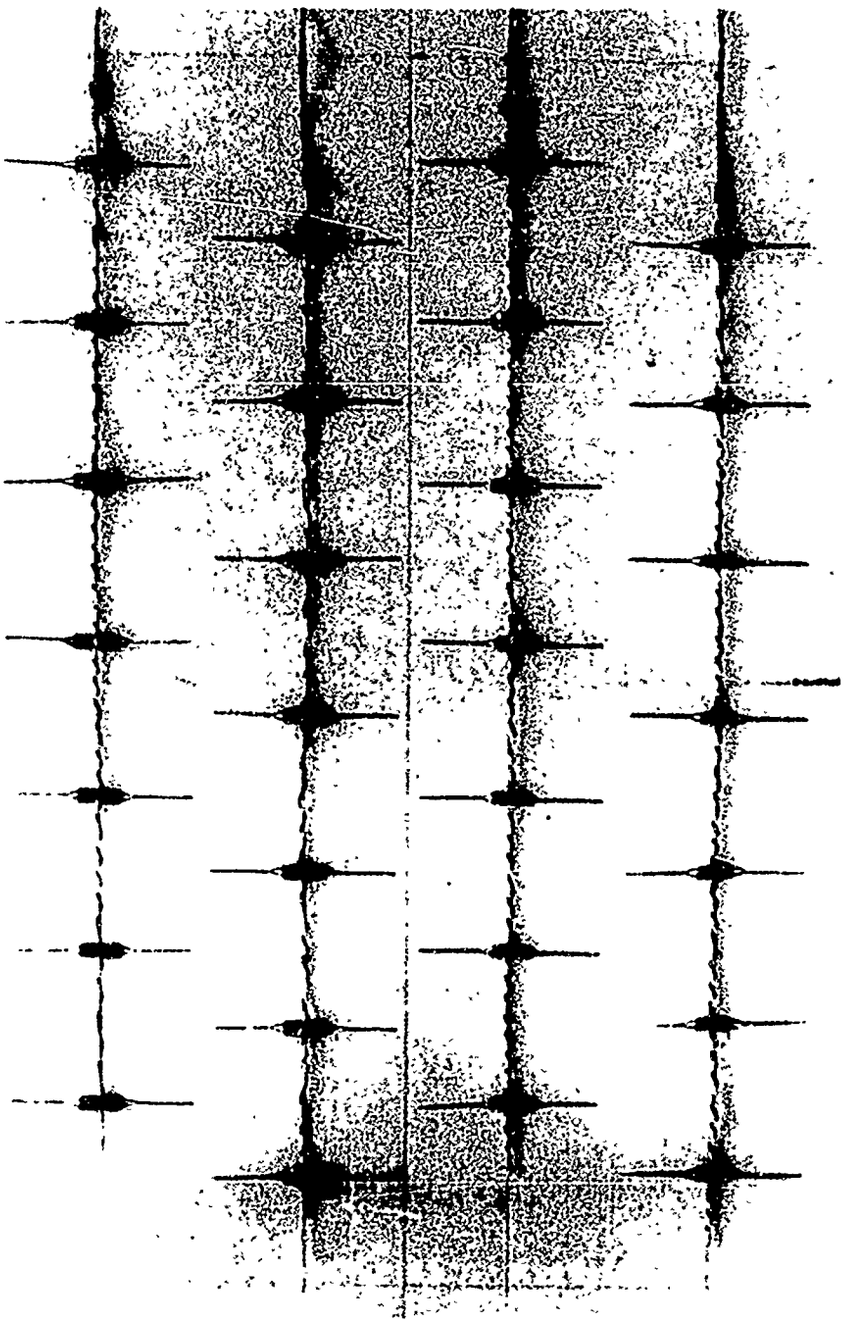

Figure 30. An Array of Half-Wave Dipoles Terminated in a Bridge-Rectifier Array of Point-Contact Silicon Diodes. Reflecting Plate is Located at a $\lambda/4$ Distance Behind the Diodes

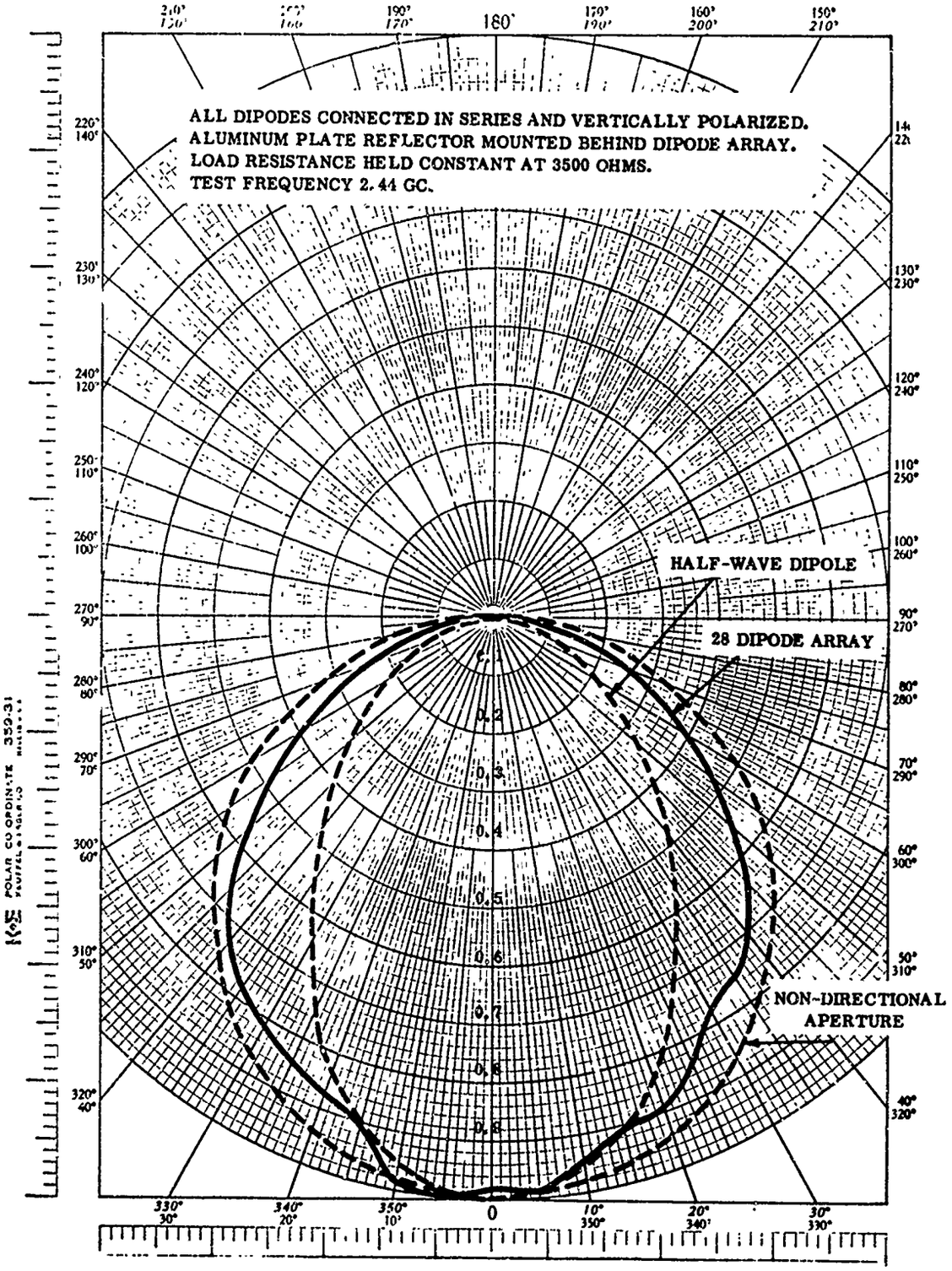

Figure 31. Directivity of the Half-Wave Dipole Array Shown in Figure 30. Directivity was Essentially the Same About Both Axes of Rotation.

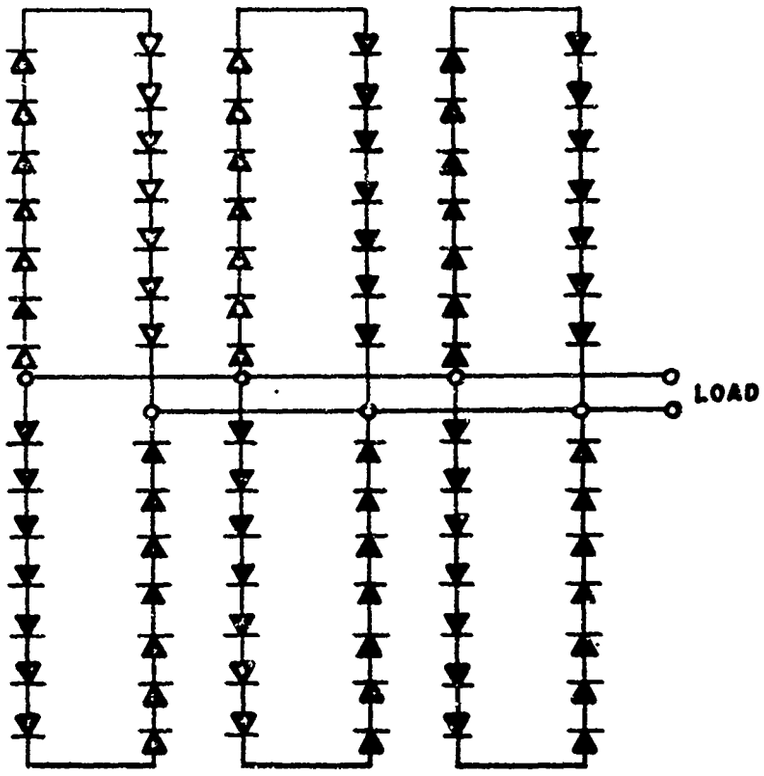

Figure 32. Schematic Drawing Showing Arrangement of Dipoles and Interconnections within a Diode Module.

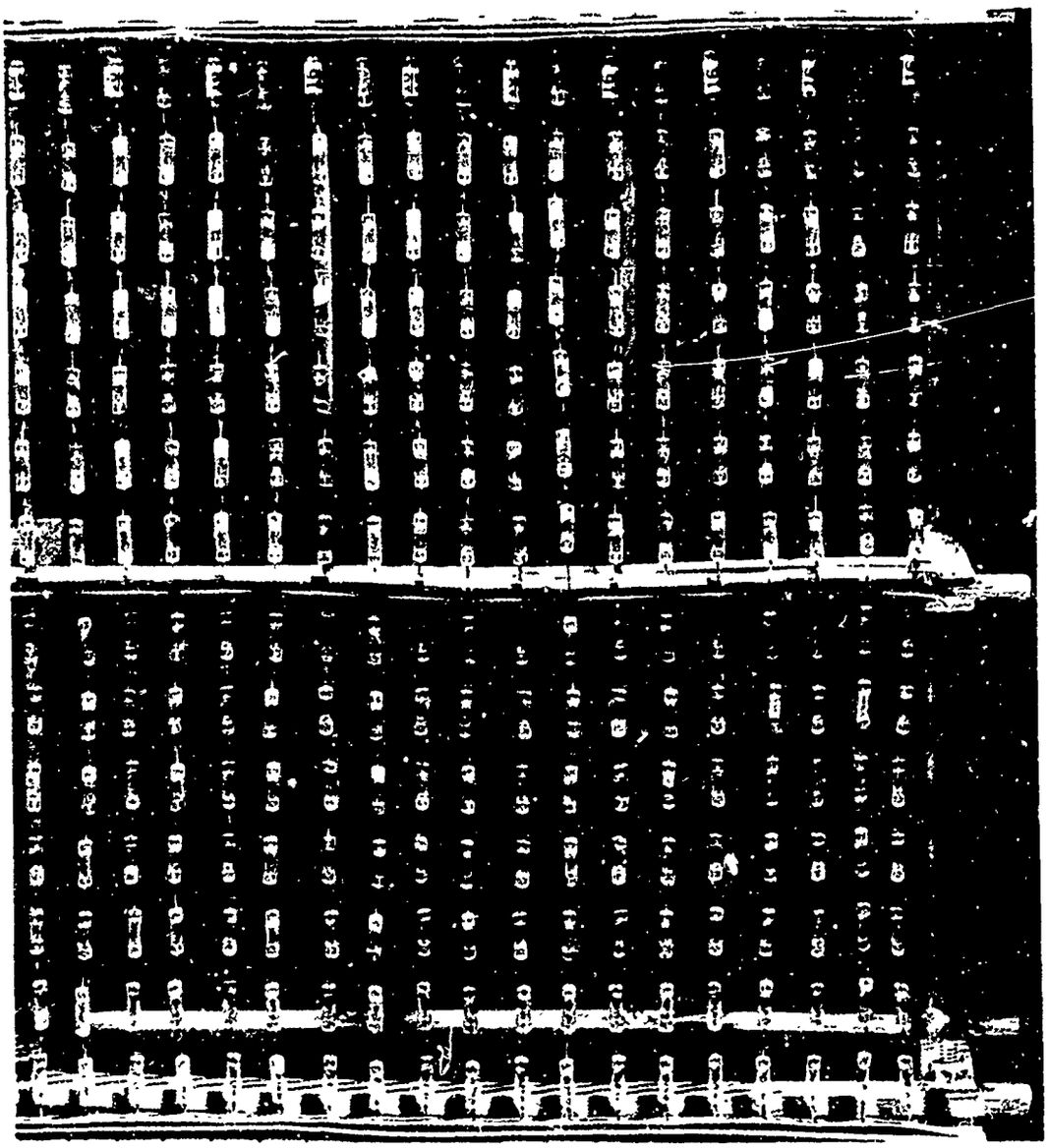

Figure 33. Photograph of One of the Sixteen 289 Element Diode Modules which Made Up the Rectenna

Another approach to the combined antenna-rectifier problem would have been to terminate each dipole of a half-wave diode array with a large number of rectifier diodes to make the power handling capability comparable to the approach that was used. This approach was unattractive because of the cooling problem that might arise with such a high packing density of diodes. The antenna is so placed that the rectifier diodes are automatically cooled by the downwash of the helicopter rotor, but since the antenna is located toward the center of the rotor where the downwash velocity is low, it is desirable to deploy the diodes in such a manner as to maximize the exposed area of each diode and its leads.

The combined antenna rectifier approach that was used was not only a key element in making the first microwave-powered helicopter flights a success, but because of a recent breakthrough in the specific weight of semiconductor diodes, it will undoubtedly be the continuing approach for aerospace applications. The specific weights of the new Schottky barrier diodes are less than one-half pound per kilowatt making it possible to think in terms of specific weights of the combined antenna and rectifier of less than two pounds per kilowatt. Another aspect of these new diodes is their higher efficiency and their much smaller size in relationship to their power rating which will reduce their drag in wind and in the slipstream of higher-velocity rotor downwashes.

Instead of being a source of unreliability, the large numbers of diodes employed actually provide a high degree of reliability through the redundant nature of the parallel series connections within each module. As shown in Figures 32 and 33, each leg of one of the twenty-eight element bridge rectifiers contains seven diodes. If one of these shorts out, the normal voltage drop across this diode is divided among the six remaining diodes. If one of the diodes opens up, the strings are in such close proximity to each other that adjacent strings of other bridge rectifier assemblies take the additional load. It is possible to have a score of open connections or shorted diodes in the individual strings, loacted at random throughout the antenna, without a severe degradation in performance.

The module concept that was employed in the construction of the microwave-powered helicopter antenna provided a high degree of flexibility in matching the antenna to the motor load. The performance of the individual modules themselves are highly insensitive to a wide range of loads applied to them, as shown in Figure 34, in which relative dc power output for fixed rf input is plotted as a function of load resistance. A very noncritical optimum performance of about thirty volts and half an ampere was indicated for each module. It was therefore convenient to form sub-groups by combining four modules in parallel and then to connect four of these sub-groups in series to provide two amperes of current at a nominal potential of 120 volts.

The vibration problems of such an antenna are severe, especially when the helicopter with its rigid rotor is tied into a tethering system and there is a brisk wind. A moment is applied to the shaft each time one of the rotor blades comes into the wind, and the flexibility of the tethering system is such as to allow a substantial deflection of the helicopter around one of its axes. The result is a whipping action which is transmitted to the antenna. Slow motion pictures of some of the original structures showed large amplitude vibrations of sections of the diode assemblies within the modules. Eventually, the strong welded joints between the diodes would break. This problem was eventually solved by better support of the diodes within the antenna, and a bracing of the antenna with either balsa strips or nylon line. These materials also introduce a high damping coefficient to help damp out higher frequency modes of oscillation. The effectiveness of this approach was demonstrated by the ten hour continuous operation of the microwave-powered helicopter with only one unimportant weld break occurring even though brisk winds and moderate rainfall were encountered during a substantial portion of the run.

The need for strong weld joints was realized when we first started working with these diodes and accordingly an investigation was started to determine a reliable method of welding these diodes. Test welds were made on several types of resistance welders. AC welders were found superior to capacitor storage bank welders and the most reliable welds were obtained on a Slee resistance welder containing an electronic means of insuring that all welding charges at a particular setting of the

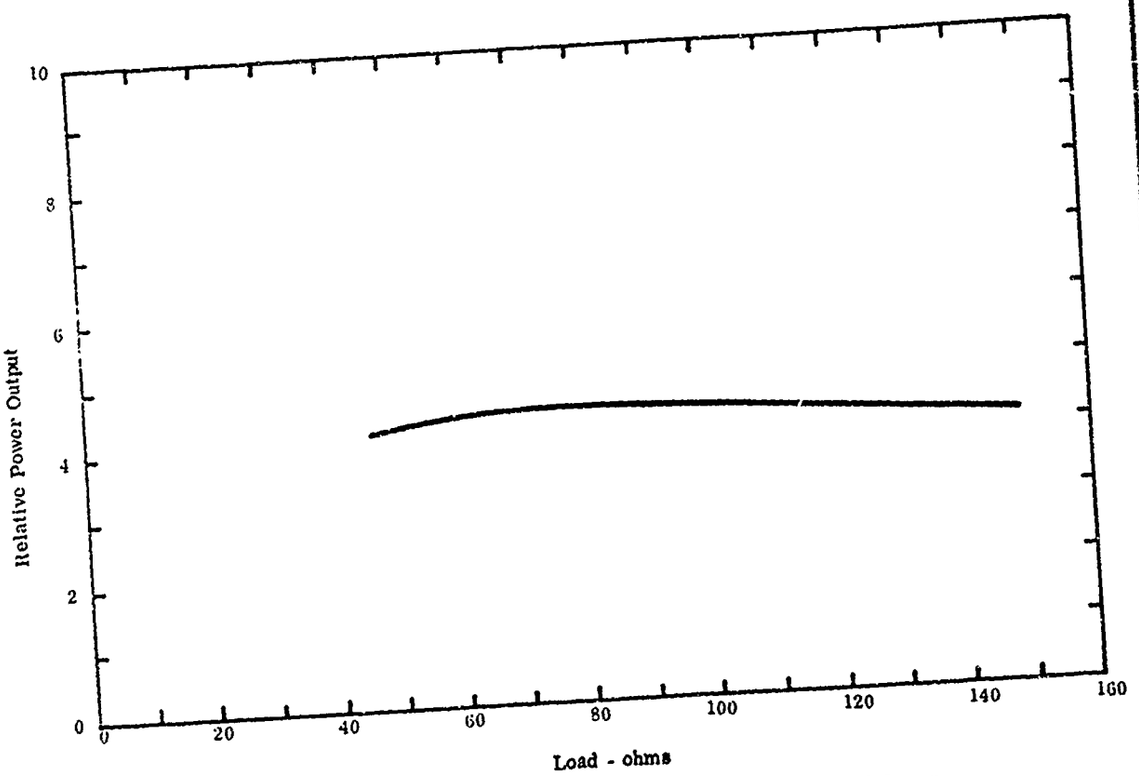

Figure 34. Experimental Data Showing the Non-Critical Dependence of the DC Power Output of a Typical Rectenna Module Upon the Resistive Load Connected to Its Terminals

machine were identical. Figure 35 is an enlarged photograph of a typical weld that has been tested to failure in tension. This sample weld is between two pieces of .020 inch diameter copper plated glass sealing alloy. The weld failed when it was subjected to 92% of the stress required to break the wire itself. A plot of the breaking strength in tension of 21 of these sample welds is included as Figure 36. Note the average breaking strength of the welds is 91% of the wire itself and that none of the welds exhibited breaking strengths of less than 22 pounds.

Figure 37 is an enlargement of test #15 in which the wire was weaker than the weld. One end of the broken wire can be seen along the side of the weld; note the necking down.

Before the diodes are resistance welded together to form the arms of the bridges, the leads projecting out each end of the .100 inch OD x .300 inch long glass envelope are cut to appropriate lengths. The units in the center of the bridge and the ones on the ends have different-length leads from the ones between these points. An air actuated press was tooled up for the job of cutting these leads. The cutting fixture, Figure 38, is capable of being adjusted to accurately cut the different lead lengths. The precise job that this tooling performs makes it possible to accurately jig the diodes in position during welding.

With the basic welding process firmly in hand, a welding jig was designed to hold 14 of the diodes in the proper welding position. The lower half of this fixture is shown being loaded in Figure 39. The technician is placing the tenth of the fourteen separate diodes in the welding fixture. After all the diodes are in place, the assembly is visually checked. The top half of the welding fixture is then lowered and tightly clamped down with the two knurled nuts. A second man performs the welding operation while the first technician arranges the next set of fourteen diodes for loading into the fixture. The technician doing the actual resistance welding, Figure 40 also

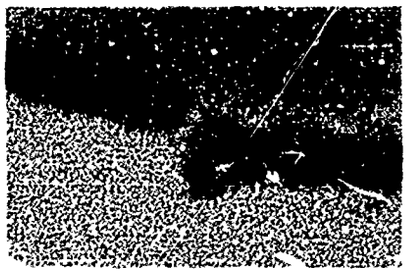

Figure 35. Typical Sample Weld Used in Rectenna Construction Tested to Failure at 92% of the Wire Strength - Enlarged 7 Times

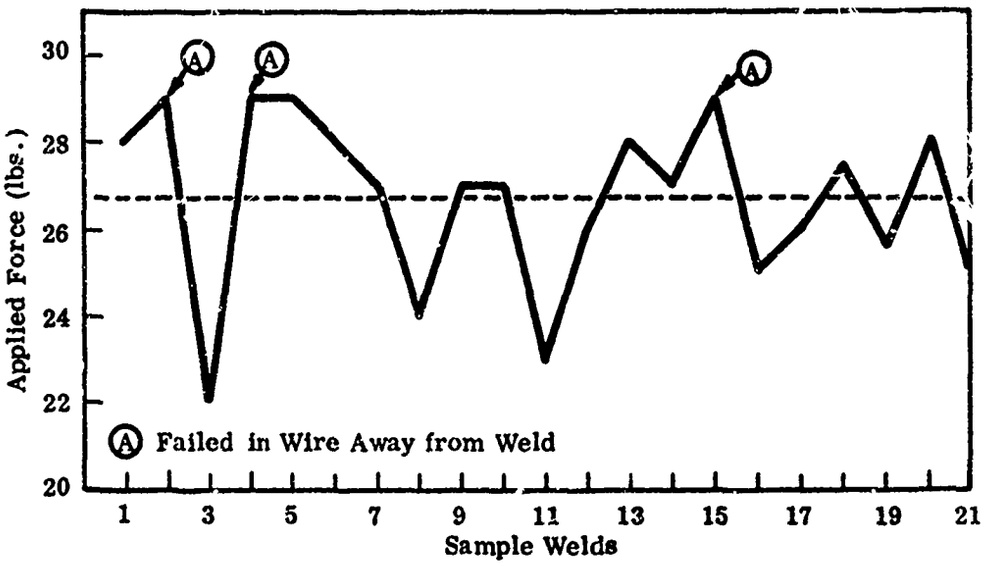

Figure 36. A Plot of the Tensile Strength of 21 Sample Welds.

Figure 37. One of Several Sample Welds which Tested Stronger than the Wire Itself. The End of the Wire at Its Failure Point is Shown Above the Weld Junction - Enlarged 7 Times.

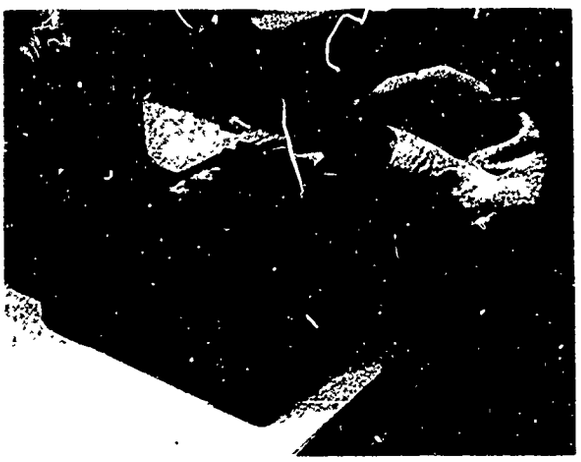

Figure 38. A Diode in Position for Lead Trimming

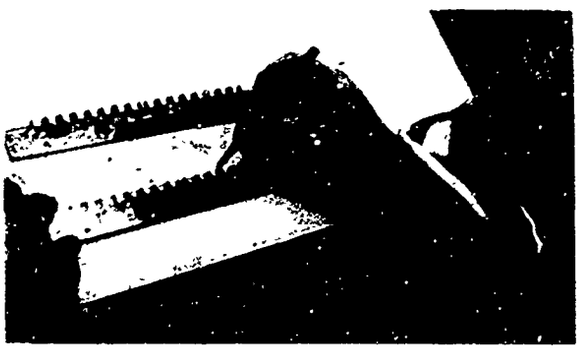

Figure 39. Diodes being Loaded into Welding Fixture

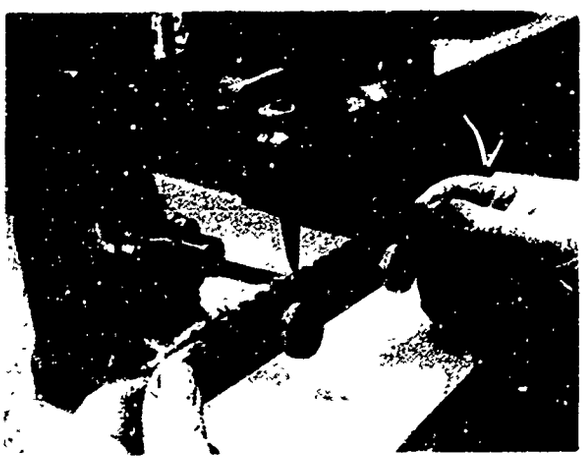

Figure 40. A String of Fourteen Diodes Being Resistance Welded

inspects the orientation of the diodes as a further check on their position.

The output product of this team is referred to as "diode strings". There are four of these strings in each bridge-type rectifier. Ten of these bridges are joined together at their ends with light plastic strips. Next, .015 inch diameter bus bars are welded to the center of the bridges so as to couple the outputs of the bridges in parallel. Small sleeves of teflon tubing are slipped over the busses where they might have a tendency to short. A second redundant bus is welded to every third or fourth bridge to counteract any bus bar joints which might open up during a windy flight.

RF Matching Network and Diode Supporting Structures

The diode network is matched to the rf energy with 13-1/8" diameter aluminum tubes spaced on 2" centers and mounted in a plane 2" in front of the diode network. These tubes in addition to their electronic matching duties serve to provide mechanical support to the rectenna. The view of the underside of the rectenna in Figure 41 shows how these tubes are in turn supported from the main center tube by a 3/8" OD aluminum strut. Also shown is the "X" brace used to provide additional support. This member is fabricated of 1/8" thick balsa and is covered with silkspan. Figure 42 is a top view of the rectenna.

The completed rectenna weighs 2.05 pounds. The diodes alone weigh one pound. The remaining weight is distributed between the matching structure and the supporting members.

The 1/8" diameter rods separated by a distance of 2" form a so-called "inductive grating" whose equivalent circuit may be represented as shown in Figure 40a.

Once this equivalent circuit is established, it may then be combined with the diode array and the characteristic impedance of space to form an over-all equivalent circuit as shown in Figure 40b. There are four circuit elements of importance: (1) the inductive grating itself; (2) the section of space of length ℓ; (3) the diode array; and (4) the terminating impedance of space.

The diode array, primarily because the DC load is in the low resistance range, appears as a low RF impedance relative to the characteristic impedance Z_o of space (377 ohms per square). The low impedance of the diode array minimizes the amount of RF energy which gets into the equivalent circuit element Z_o, at the extreme right of Figure 40b.

During the course of the work, the impedance Z_d of the diode array was never accurately measured. It was early determined that the VSWR, measured by means of a probe placed in front of the array, depended upon the RF power level incident upon the array and increased rapidly as the DC power output of the diode array was observed to saturate. VSWR's of as high as 10 were obtained under saturated power output conditions.

It may be appreciated that accurate measurements of VSWR and phase position of the VSWR minimum would involve making these measurements in a high power density beam. Although an accurate experimental setup provided with remote control was planned, the inductive grating was introduced before this was accomplished. The inductive grating was found to have a beneficial effect upon improving the match to the rectenna

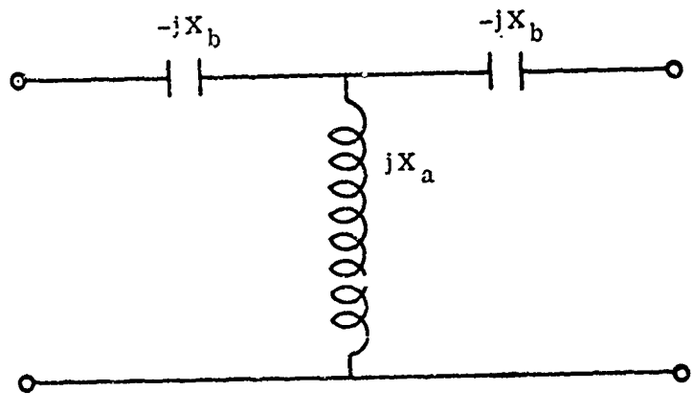

Figure 40(a). Equivalent Circuit of Bar Inductive Grating

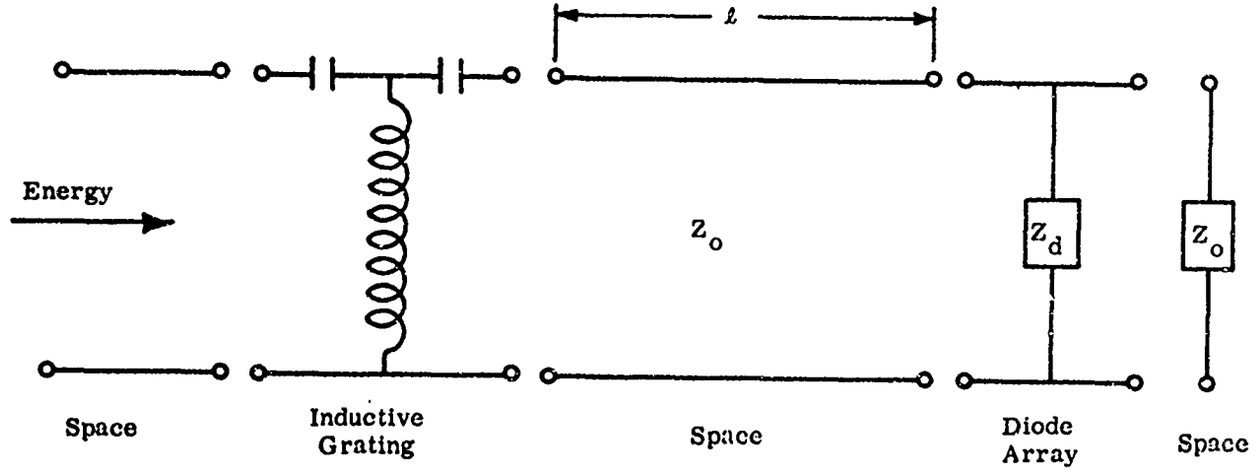

Figure 40(b). Equivalent Circuit of Rectenna

and in increasing the saturated DC output. The spacing between the rods of the grating was empirically set to produce the maximum DC power output. This condition did not result in a unity standing wave ratio and considerable RF power was still reflected. However, the rectenna was made adequate for use in the microwave-powered helicopter.

With the inductive grating parameters adjusted for optimum rectenna performance, the equivalent electrical parameters of Fig. 40a as computed from section 5.21 of Marcuvitz "Waveguide Handbook", McGraw-Hill, were --

$$j X_a = j 0.7 Z_o, \text{ and } -j X_b = -j .01 Z_o.$$

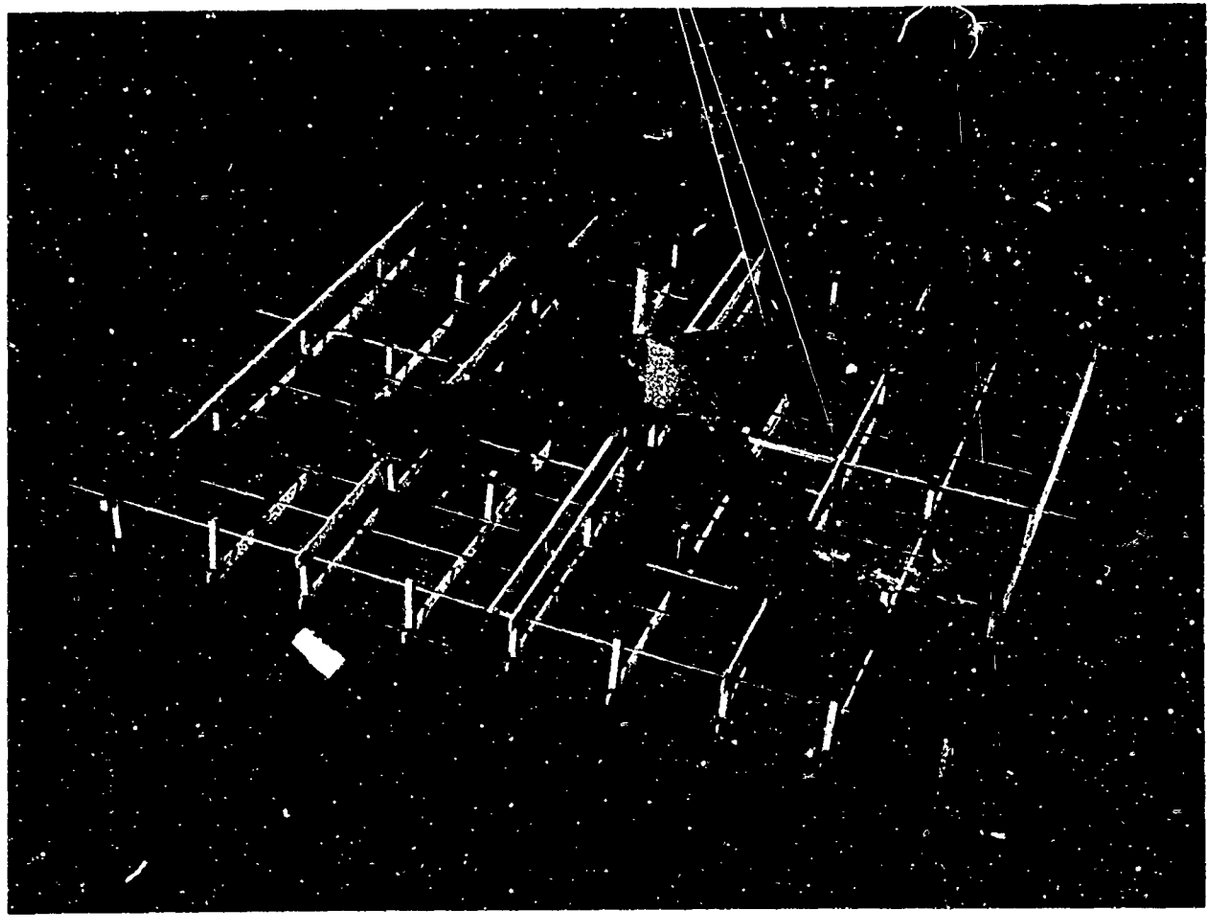

Figure 41. A View of the Receiving Surface of the Rectenna Showing the Bracing and Matching Structure

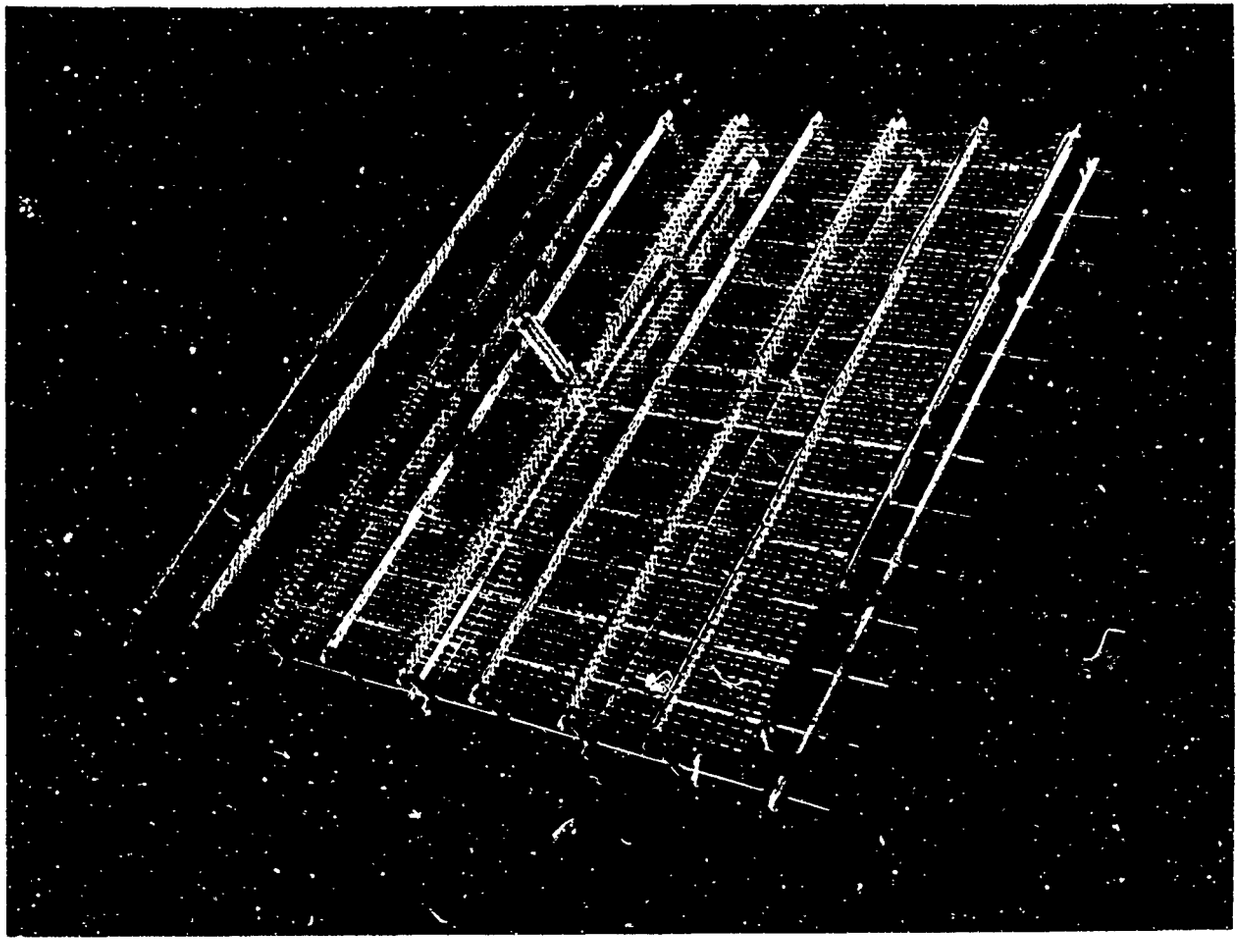

Figure 42. A Top View of the Rectenna

3.5 THE MICROWAVE BEAM

The microwave beam system which has been used for the microwave-powered helicopter flights is a modification of the apparatus employed for the first demonstration of the efficient transfer of meaningful amounts of power in May of 1963. The major modification was to shift the second focal point of the system from 25 feet to 50 feet. The ellipsoidal reflector was therefore not of optimum design, but the energy distribution around the second focal point was sufficiently satisfactory for the microwave-powered helicopter demonstration.

Because of the still rather new aspect of an antenna system designed for power transmission, it may be desirable to present some background information on the subject. The background information that will be discussed is of both an experimental and theoretical nature.

From a theoretical point of view, it is desirable to start with an ellipse as shown in Figure 43. The ellipse has two interesting properties when used in connection with the focusing of microwave energy. The first property is that any ray of energy which is radiated from the first focal point, regardless of the direction of radiation, will arrive at the second focal point. The second property is that no matter what direction the ray takes from the source of illumination at the first focal point the traversed distance to the second focal point is always the same. Thus all rays of energy radiated in phase from the first focal point will arrive in phase at the second focal point. Because all rays are in phase at the second or receiving focal point they must also be in phase on the arc of a spherical surface drawn with the center at the second focal point. This means that the phase front of a beam, originating from a point source, is spherical.

Figure 44 gives the dimensions of an ellipse, using common ratios of antenna diameter to focal distance, which would be characteristic of transferring power over a distance of 10 miles. The construction of such an ellipse, of course, is not practical nor necessary, and the question immediately arises as to how much of the

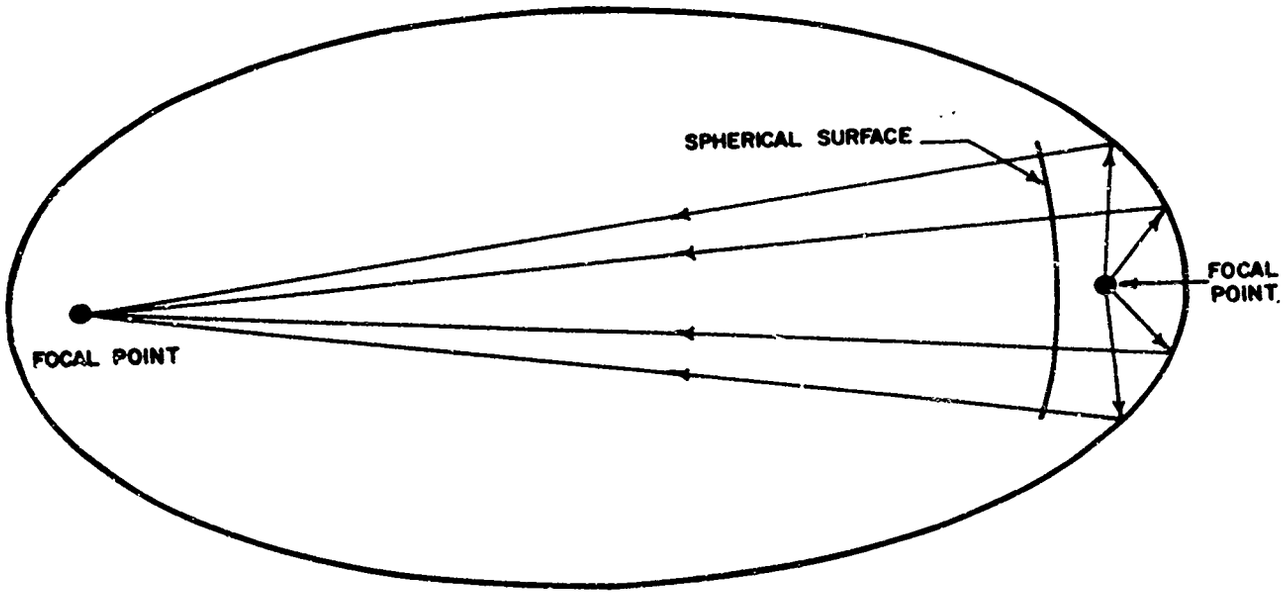

Figure 43 The Basic Ellipse Geometry Used in Designing Microwave Transmission Systems.

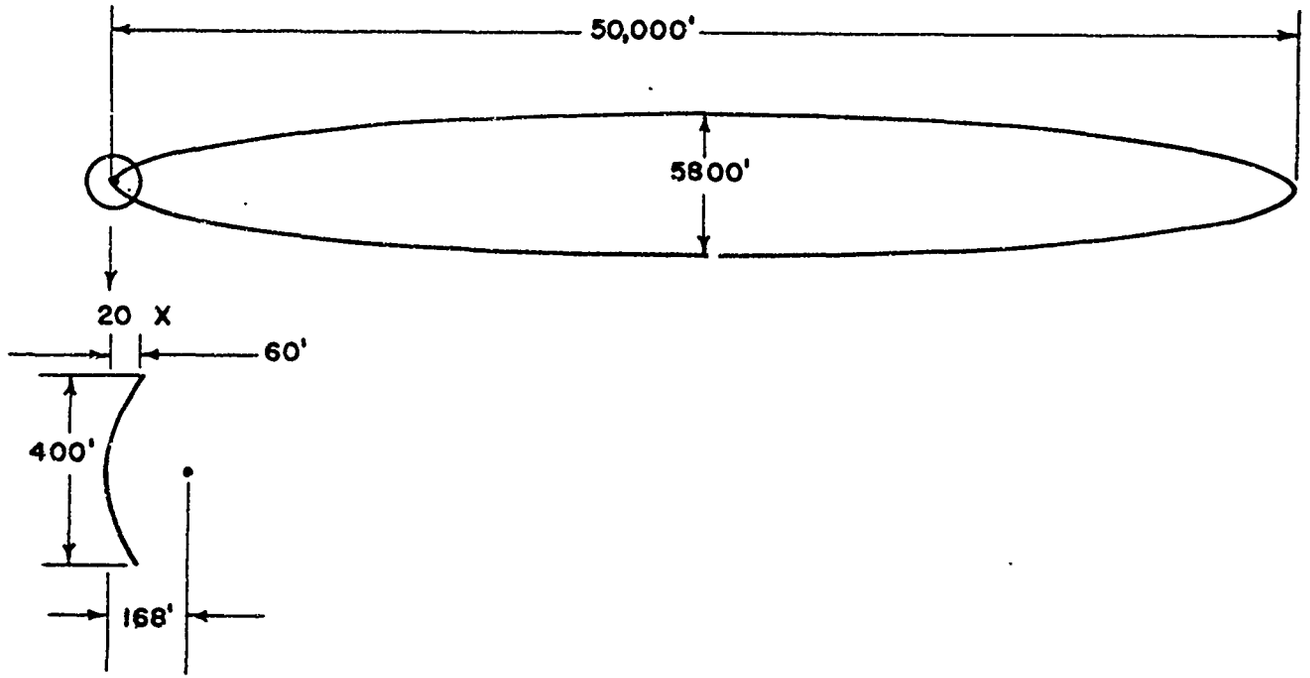

Figure 44 Dimensions of an Ellipsoid Suitable for Transmitting Power at a 10 cm Wavelength to a 100 Ft. Receiving Aperture Over a Distance of Ten Miles.

ellipsoid in the region of the source focal point is necessary in order to focus the energy near the second or receiving focal point. To evaluate the size of the antenna aperture needed for a given application we must take the laws of diffraction into account. These can be most easily applied to our problem by the geometrical construction shown in Figure 45. In this illustration the phase front established by the transmitting antenna is divided into a large number of radiation vectors of equal amplitude and phase. Uniform illumination is assumed. It is then observed how these vectors add or cancel in the region of the receiving point. To make the principle easier to understand a line source rather than a point source is first considered.

Referring to Figure 45, it is noted that point A on the receiving surface ABC is equidistant from all points on the circular wave front. All radiation vectors are therefore in phase and the situation is that shown in A of Figure 45. At point B, the vectors will be out of phase to some degree and the situation is that shown in B of Figure 45. Finally, at point C there is a situation in which the vectors cancel to produce a null point in the illumination of the plane ABC.

A simple analysis shows that the illumination intensity of the area in the region of the focal point follows the relationship --

$$P = P_m \frac{\sin X}{X} \quad \text{where,} \tag{1}$$

P_m = maximum power density at $X = 0$, and

$$X = \frac{d D_t \Pi}{h \lambda} \quad \text{where}$$

h = separation between transmitting and receiving antennas

λ = wavelength of electromagnetic radiation

D_t = transmitting antenna diameter

d = distance off axis of point under consideration.

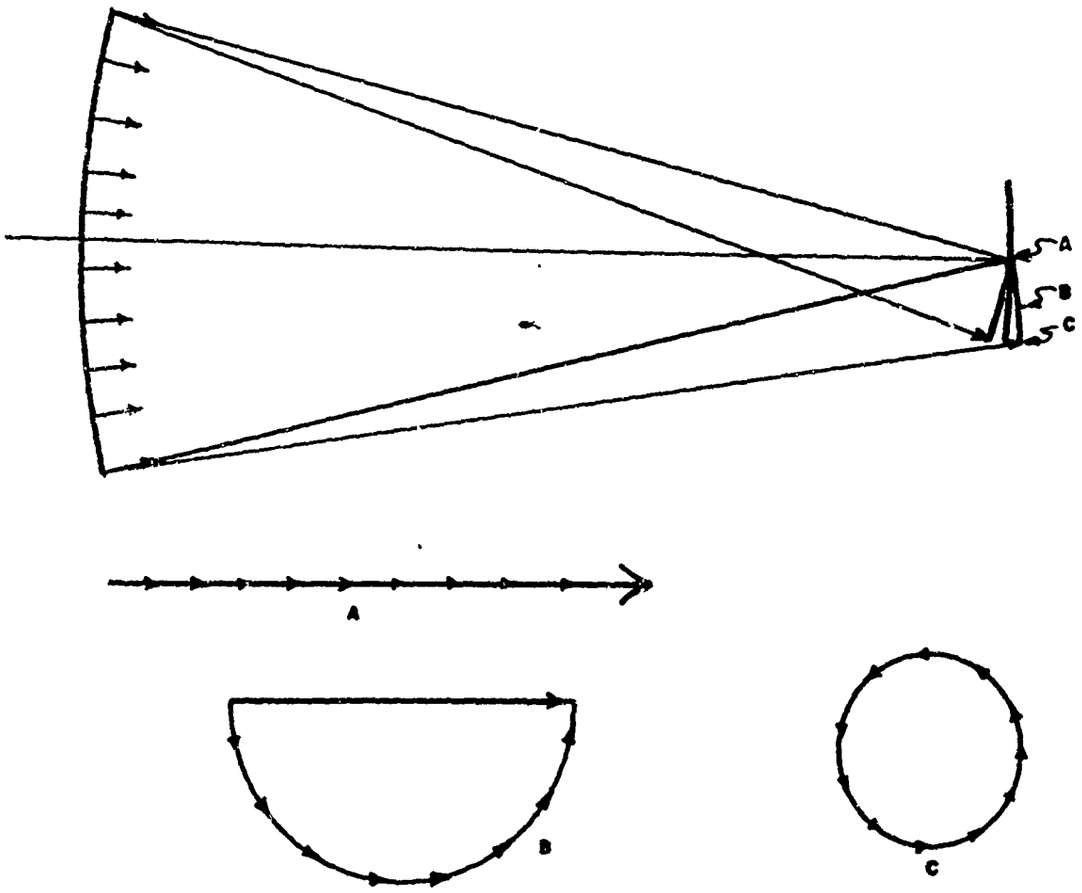

Figure 45 Geometrical Construction Illustrating How the Radiation Add Up to Produce a Variation of Power Density in the Region of the Receiving Aperture.

The $\frac{\sin X}{X}$ function is shown in Figure 46. It will be noted that the first null point occurs at $d = \frac{h \lambda}{D_t}$.

The situation is more complicated in the case of a point source illuminating an ellipsoidal reflector uniformly. In this case, it is necessary to find the solution in terms of a Bessel function. For such a point source of illumination, the illumination in the region of the receiving focal point varies as a function of distance from the axis as shown in Figure 47.

The relationship between the distance h between the transmitting and receiving point, the diameters D_s and D_r of the transmitting and receiving aperture respectively, and the free space λ wavelength is shown in Equation (2).

$$P = P_m \left[\frac{2 J_1 (X)}{X}\right]^2 \quad \text{where} \qquad (2)$$

P_m and X are as previously defined and J_1 is the Bessel function of first kind, order 1. In this case, the first null point occurs at $d = \frac{1.22 h \lambda}{D_t}$.

Although the theoretical approach is taken directly from optical theory, there has been very little experimental application of these laws to microwave optics for the case in which it is desired to have the energy at the second focal point concentrated into an area considerably smaller than that of the transmitting reflector. For this reason, a bench setup was made at a wavelength of eight millimeters for experimentally testing out these relationships. The physical setup is shown in Figure 48. In this experimental setup, an ellipsoidal reflector 9.5 inches in diameter was used to establish the convergent beam which was focused at a distance 23.9 inches from the center of the ellipsoidal reflector. The power distribution was probed around the second focal point. The distribution together with the theoretical prediction distribution is shown in Figure 49. The agreement between experiment and theory seems to be quite good. The efficiency of power transfer in this experimental setup was also quite good. It was possible to collect with the collecting horn shown in Figure 48, 52% of the energy flowing through the transmitting waveguide.

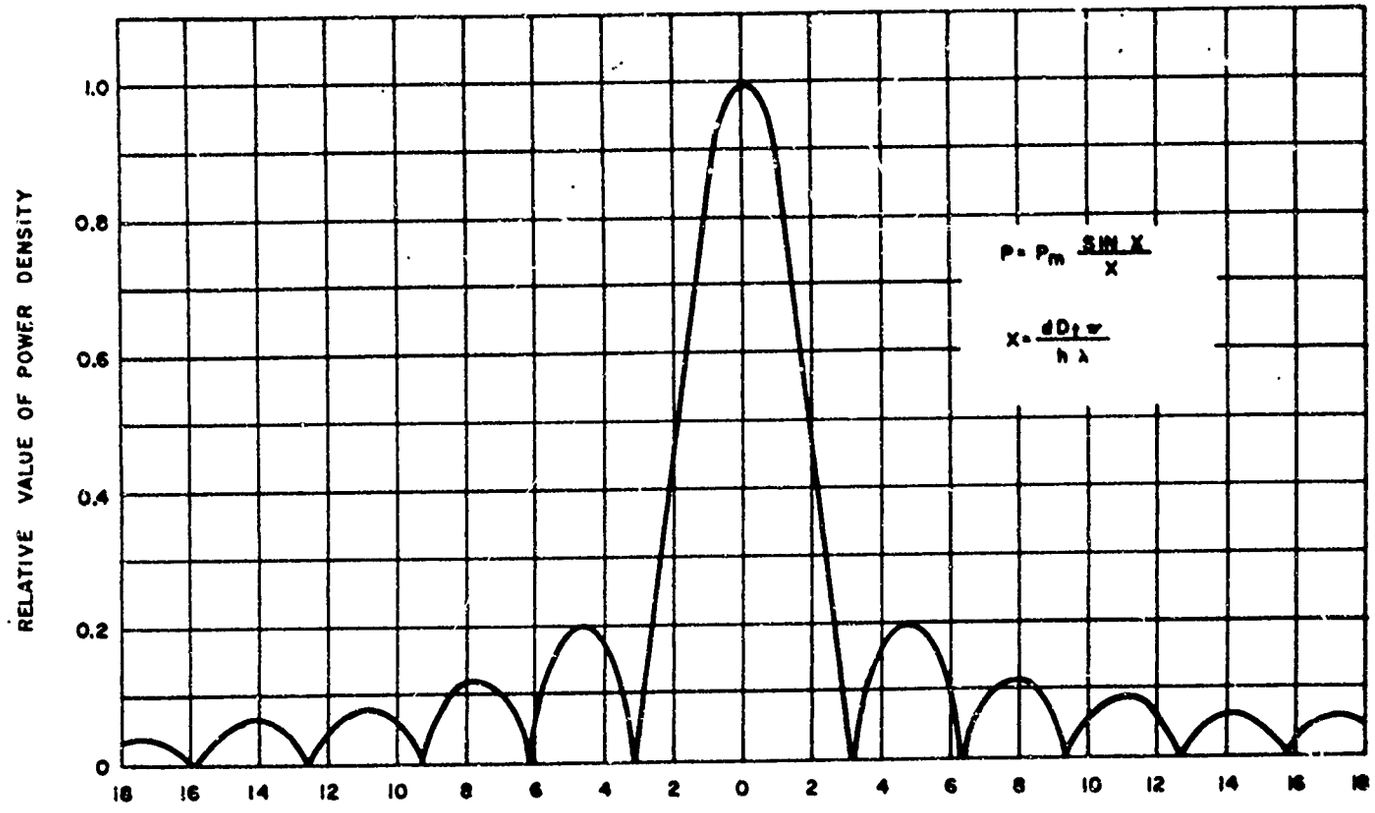

Figure 46 The $\frac{\text{SIN X}}{\text{X}}$ Function Characteristic of the Power Density Distribution in the Region of the Receiving Aperture for a Line Source of Radiation Employing a Reflection Elliptical in Configuration.

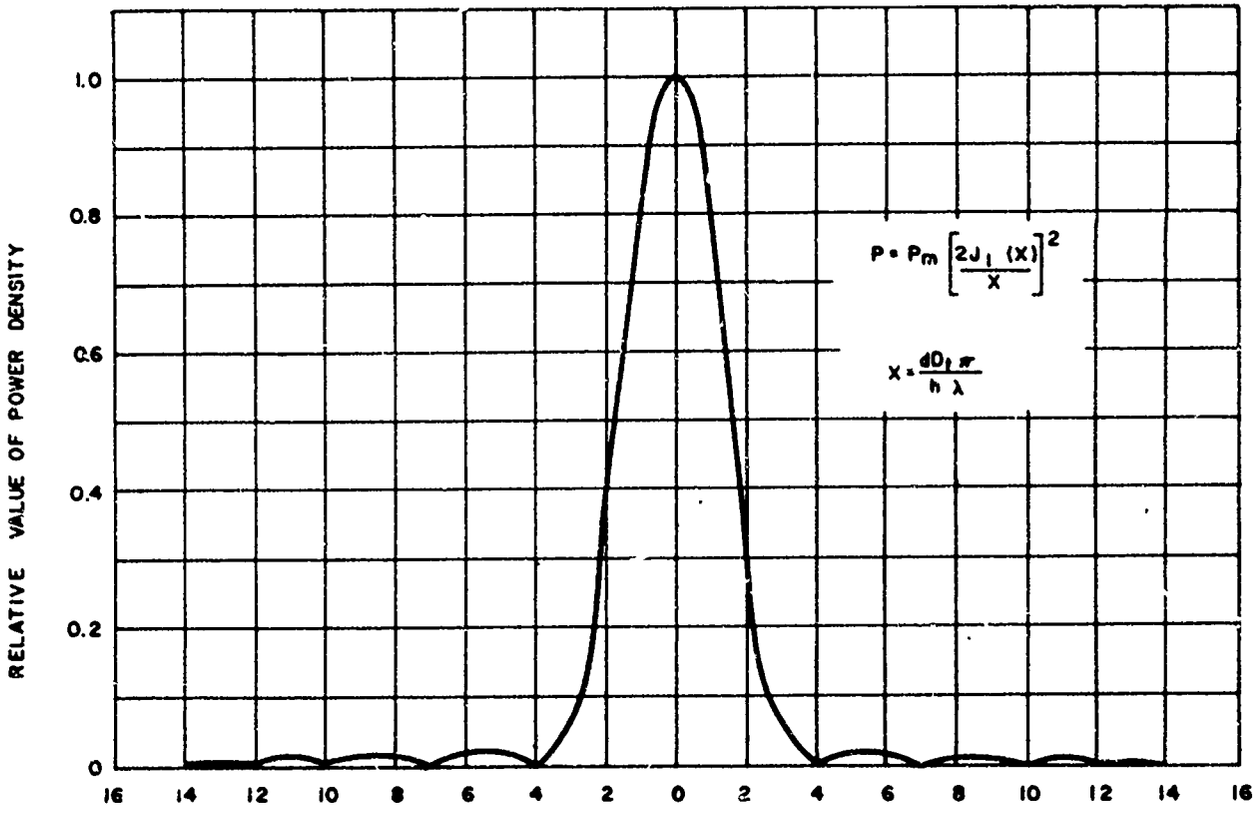

Figure 47 A Plot of the $\frac{2 J_1(X)}{X}$ Function Giving the Power Density in the Region of the Receiving Aperture for a Point Source of Radiation Employing an Ellipsoidal Reflector.

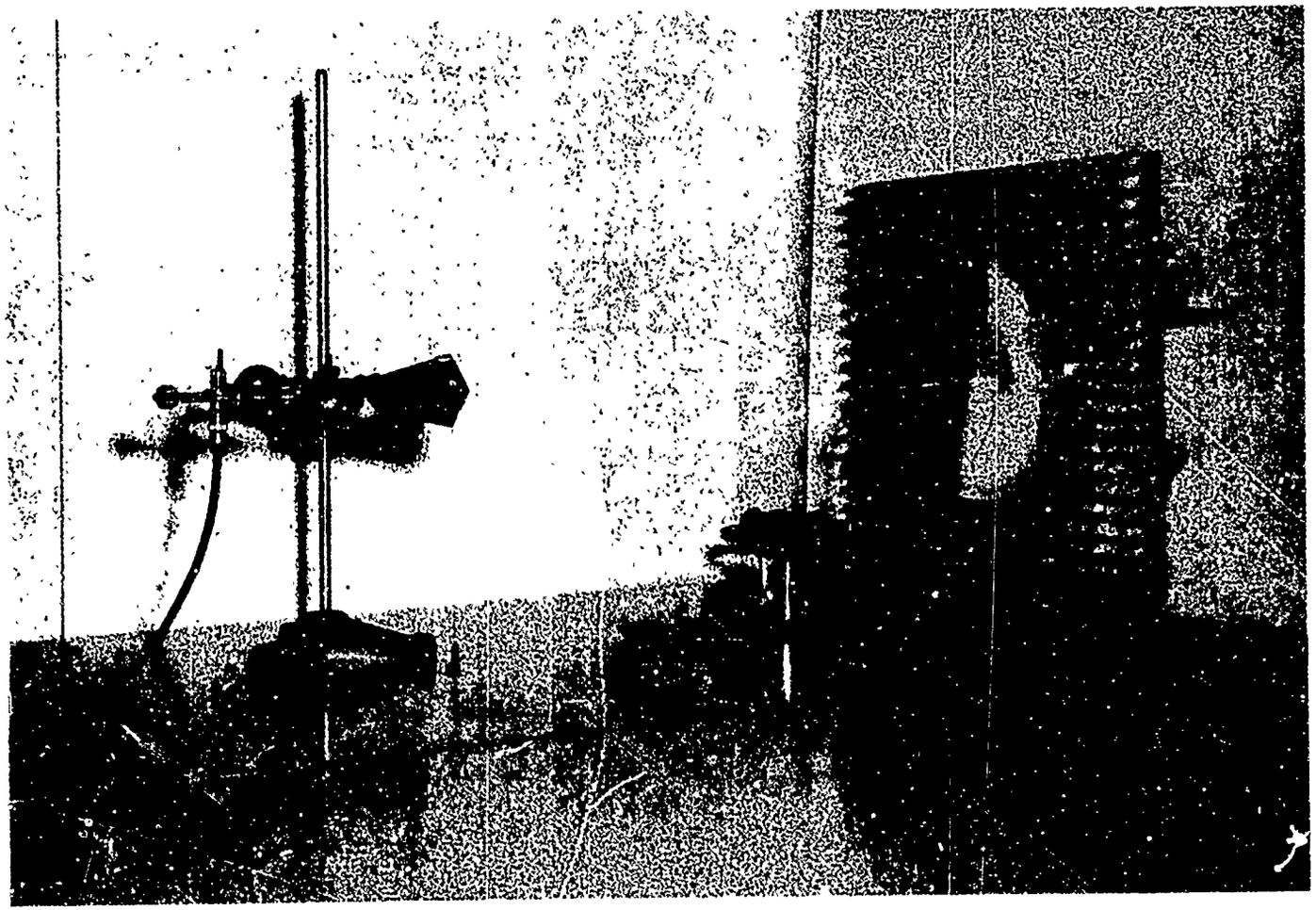

Figure 48. 8 MM Scale Model of the Lens System Used in the Power Transfer Experiment of Figure 50.

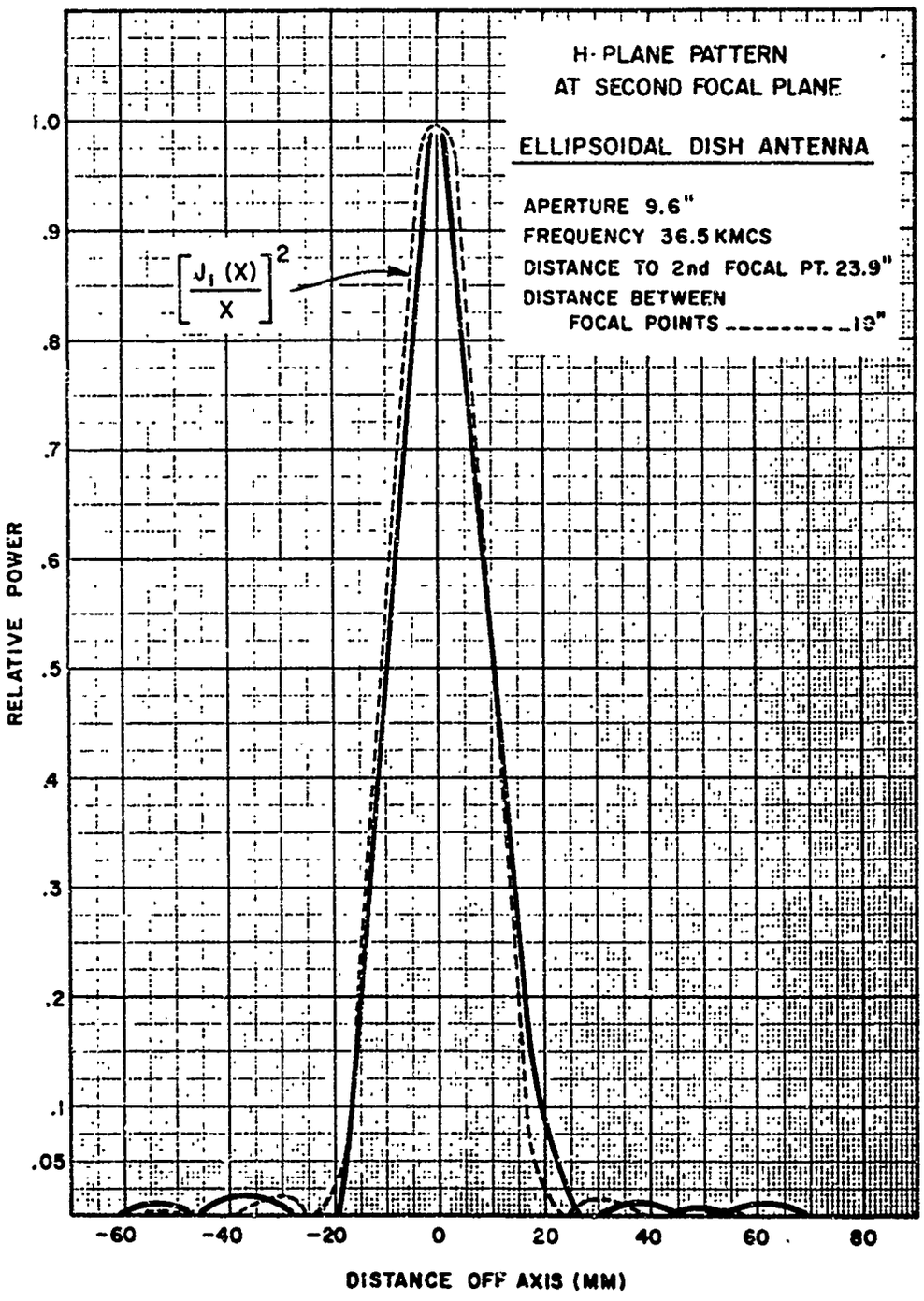

Figure 49. Above Pattern was Obtained with a Section of RG 96/U Waveguide Used as a Pattern Probe in Place of the Diagonal Horn in Figure 48. The Theoretical Distribution for a Uniformly Illuminated Transmitting Aperture of the Same Size and Shape is Shown for Comparison.

This experimental setup was then scaled to a wavelength of 12 centimeters as shown in Figure 50. This apparatus was used to carry out early experiments in the efficient transfer of electrical power by microwaves. In these experiments, power was first converted into microwave power, the microwave power was transmitted and collected with an efficiency of 50%, and then rectified with an efficiency of 50%. The rectified power of 100 watts was used to drive an electrical motor.

Because of the existence of this apparatus, it was of interest to determine if it could be suitably modified to meet the requirements of the microwave-powered helicopter experiment. This investigation consisted of changing the focal distance F_1 and examining the rf pattern at F_2, as shown in Figure 51. A plot of the rf field pattern at a distance of 45 feet from the transmitting aperture as a function of the focal length F_1 of the transmitter feed horn is shown in Figure 52. Although the field patterns were taken at 45 feet instead of 50 feet because of physical limitations which existed at the time the data was taken, there was good reason to believe that there would be no marked change in the shape of the field pattern at a distance of fifty feet. On the basis of the various patterns obtained at a focal distance, an F_1 of 52 inches was used for the microwave beam for the microwave-powered helicopter experiment.

The quantity of microwave power as measured at the output of the magnetron that was used for the helicopter experiment varied from a minimum of three kilowatts to a maximum of five kilowatts. Thus the over-all transmission efficiency was comparatively low, but the demonstration of high transmission efficiency was not the prime objective of the experiment. Much better transmission efficiencies have been demonstrated in the May 1963 experiments previously referred to.

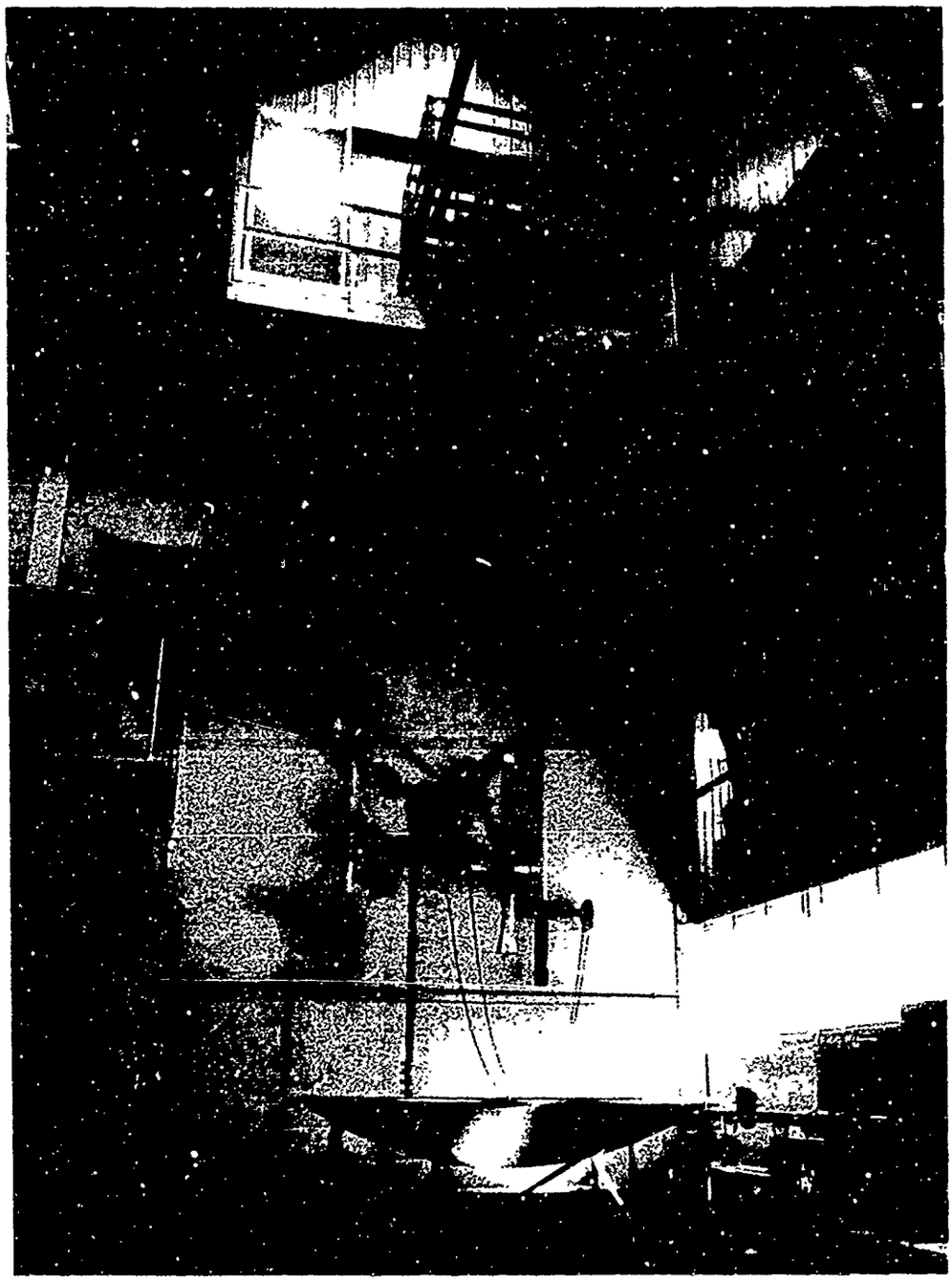

Figure 50. Experiment in Power Transfer by Microwave Beam Performed at the Raytheon Company on May 23, 1963

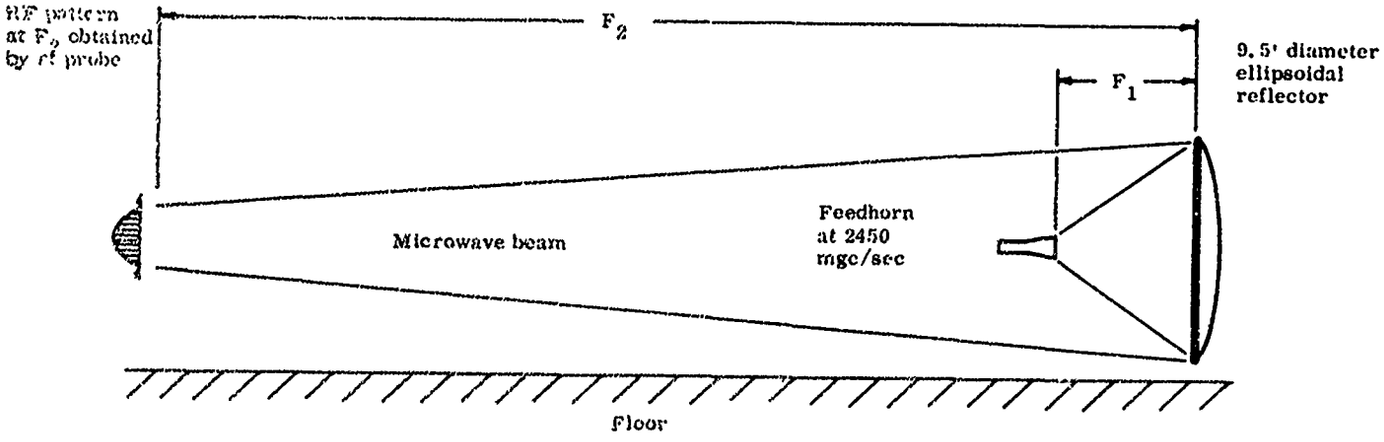

Figure 51 Horizontal Test Range for Investigating RF Patterns as a Function of F_1 and F_2.

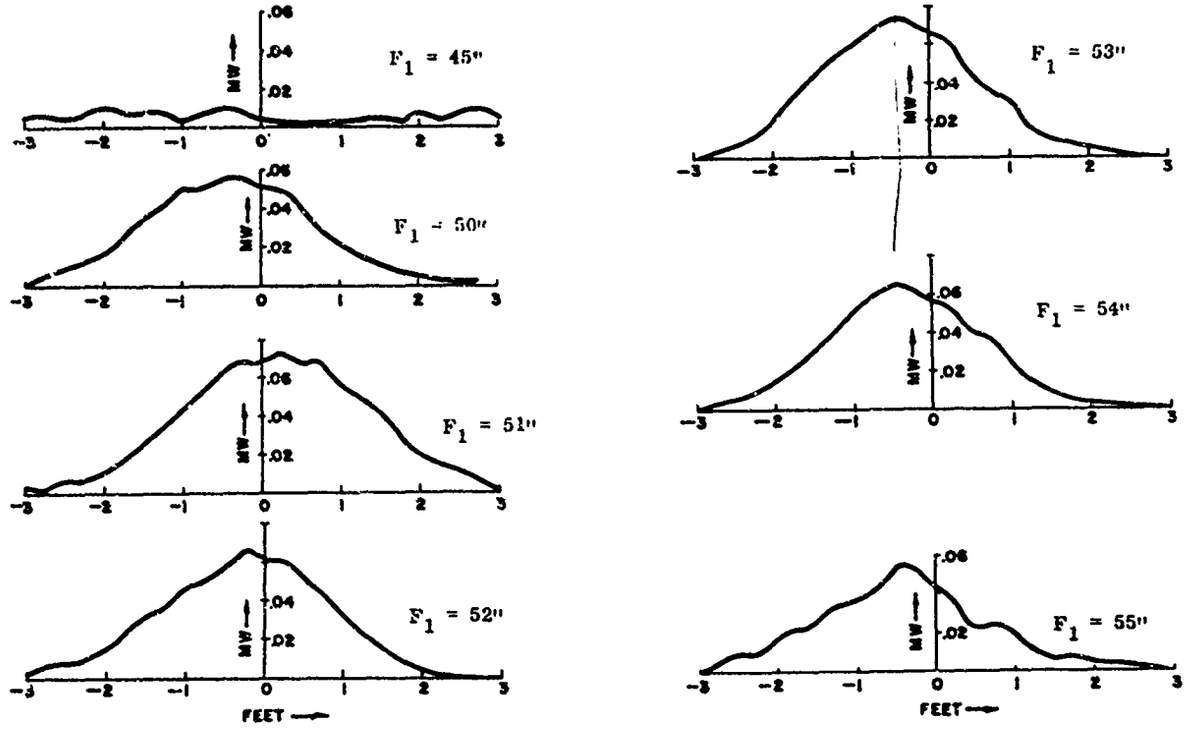

Figure 52 Microwave Beam Cross-Section Patterns at F_2 for Optimum F_1 - F_2.

4.0 CONCLUSIONS AND RECOMMENDATIONS

The most important result of the study of the microwave-powered helicopter was the demonstration that it is possible to keep a heavier-than-air vehicle aloft by power derived solely from a microwave beam for a substantial period of time and at an altitude which convincingly demonstrates the use of a microwave beam for this purpose.

Much of the activity during the study was concerned with mechanical aspects of the helicopter design. Another major portion of the activity was concerned with the undesirable interaction of the helicopter and the tethering system. In addition to this undesirable interaction, the tethering system imposed a definite limitation upon the altitude at which the microwave-powered helicopter could be flown. The helicopter itself was capable of flights of at least several thousand feet and the power level of the microwave beam system could have been increased to make flights of this altitude possible.

The next obvious stage in the development of the microwave-powered helicopter is to make it a "beam-riding" device, thus eliminating the need for the cumbersome tethering system and permitting it to ascend to much higher altitudes at which both the microwave-powered helicopter and the microwave beam system are capable of performing.

The microwave beam has sufficient information on it to provide a reference for five of the six degrees of freedom of the helicopter. Altitude is the only degree of freedom for which information is not directly available. It is therefore logical to use the beam directly as the means for controlling the position of the microwave-powered helicopter over the beam itself and a supplemental arrangement for altitude control.

It is recommended that the development of the microwave-powered helicopter be supported through its next major stage of development, namely, that of providing it with a "beam-riding" capability.

APPENDIX

SELECTED BIBLIOGRAPHY

SELECTED BIBLIOGRAPHY

1. Brown, W. C., "Experiments in the Transportation of Energy by Microwave Beam", 1964 IEEE International Convention Record, Vol. XII, Pt. 2, pp. 8-17.

2. Gessow, A., and G. C. Myers, Jr., "Aerodynamics of the Helicopter", New York: The Macmillan Company, 1952.

3. Goubau, G., and F. Schwering, "On the Guided Propagation of Electromagnetic Wave Beams", IRE Trans. on Antennas and Propagation, Vol. AP-5, April 1957, pp. 222-227.

4. George, R. H., and E. M. Sabbagh, "An Efficient Means of Converting Microwave Energy to DC, Using Semiconductor Diodes", 1963 IEEE International Convention Record, Vol. XI, Pt. 3, pp. 132-141.

5. Brown, W. C., "A Survey of the Elements of Power Transmission by a Microwave Beam", 1961 IRE International Convention Record, Vol. IX, Pt. 2, pp. 93-106.

6. Okress, E. C., W. C. Brown, T. Moreno, G. Goubau, N. I. Heenan, and R. H. George, "Microwave Power Engineering", Oct. 1964 IEEE SPECTRUM, Vol. I, No. 10, pp. 76-100.

7. Marcuvitz, N., "Waveguide Handbook, Radiation Laboratory Series, Vol. 10, New York: McGraw-Hill Book Co., Inc., 1951.